

44-05-5
Standard 150
CIT

MAY 12 1947

3 1176 00116 0689

NATIONAL ADVISORY COMMITTEE FOR AERONAUTICS

WARTIME REPORT

ORIGINALLY ISSUED
February 1942 as
Advance Restricted Report

WIND-TUNNEL TESTS OF SINGLE- AND DUAL-ROTATING PUSHER
PROPELLERS HAVING FROM THREE TO EIGHT BLADES

By David Biermann and W. H. Gray

Langley Memorial Aeronautical Laboratory
Langley Field, Va.

NACA

WASHINGTON

NACA WARTIME REPORTS are reprints of papers originally issued to provide rapid distribution of advance research results to an authorized group requiring them for the war effort. They were previously held under a security status but are now unclassified. Some of these reports were not technically edited. All have been reproduced without change in order to expedite general distribution.

L - 359

LANGLEY MEMORIAL AERONAUTICAL
LABORATORY
Langley Field, Va.

**WIND-TUNNEL TESTS OF SINGLE- AND DUAL-ROTATING PUSHER
PROPELLERS HAVING FROM THREE TO EIGHT BLADES**

By David Biermann and W. H. Gray

SUMMARY

Tests of 10-foot-diameter, single- and dual-rotating pusher propellers having from three to eight blades were conducted in the 20-foot propeller-research tunnel as a continuation of previous investigations of tractor propellers. The propellers were mounted at the rear end of a streamlined body in spinners that covered the hubs and part of the shanks. The effect of spinner length was also investigated. Blade-angle settings ranged from 20° to 70°.

The efficiencies of the dual-rotating propellers in the pusher position were about the same as for the tractor position, but the efficiencies for the single-rotating propellers were somewhat less. The gains due to dual rotation were, consequently, greater for the pusher position than for the tractor position, amounting to as much as 16 percent as compared with 8 percent. The general effects of dual rotation on other propeller characteristics were substantially the same for the pusher position as previously noted for the tractor position.

INTRODUCTION

Two previously published reports (references 1 and 2) present the results of tests on three-, four-, six-, and eight-blade, single- and dual-rotating propellers for the tractor condition. The present report presents the results of subsequent tests of the same propellers mounted in the pusher position.

The effect of an elongated spinner, both fixed and rotating, was also studied. No wing was used for the pusher tests.

APPARATUS AND METHODS

The present investigation is a continuation of others previously made in the propeller-research tunnel. (See references 1 and 2.) A detailed description of the appa-

ratus and methods will therefore not be repeated. A short description follows in order to make repeated reference to the previous reports unnecessary.

Model.-- The model used in the previous tests was turned end for end. As both ends of the body are identical, the flow over the body was similar for the tractor and pusher studies.

The six-blade (dual- and single-rotation) tests were repeated with a spinner three times as long as the short one normally used. (See fig. 1.) This spinner was so constructed and supported that it could either be fixed or free to rotate.

Propellers.-- The four-, six-, and eight-blade propellers, single- and dual-rotating, were mounted in two-, three-, or four-way hubs as the case required and spaced in tandem approximately 10 inches. (See figs. 2 and 3.) Preliminary tests were made to determine the optimum angular displacement between the front and rear propeller blades for the single-rotation tests. These tests showed no appreciable aerodynamic difference between the various spacings within a range of 30° on either direction from an equal spacing. Owing to the position of the shaft splines, equal spacing was impossible; for four-, six-, and eight-blade single-rotating propellers, the front blade therefore led the rear by 85.4° , 75.0° , and 52.5° , respectively.

The blades used for this investigation were the same as previously tested; Hamilton Standard 3155-6 and 3156-6, right-hand and left-hand, respectively. Blade-form curves are given in figure 4. Clark Y sections are incorporated throughout.

Test conditions.-- Because of the limiting tunnel speed (approximately 110 mph) and the limiting power of the drive motors (two 25-hp electric motors), the Reynolds number and the tip speed were considerably lower than those experienced in flight. The maximum propeller speed, which was 550 rpm, was obtainable only for the low blade angles and the low V/nD range of the tests. The tip speed, consequently, was below 300 feet per second, and thus the effects of compressibility could not be measured. The Reynolds number of the 0.75R section was of the order of one million.

The right-hand (front) propeller was set at oven values of blade setting for the dual-rotation tests. The left-hand (rear) was set to absorb the same power as the right-hand propeller for the peak-efficiency condition only. A plot of the angular difference between the right- and the left-hand propeller-blade settings is given in figure 5. The speed of the right- and the left-hand propellers was maintained equal throughout the tests. The test procedure was the same as that used for previous investigations in this tunnel.

RESULTS AND DISCUSSION

The measured values have been reduced to the usual coefficients of thrust, power, and propulsive efficiency.

$$C_T = \frac{\text{effective thrust}}{\rho n^2 D^4}$$

$$C_P = \frac{\text{engine power}}{\rho n^3 D^5}$$

$$\eta = \frac{C_T}{C_P} \frac{V}{nD}$$

$$C_s = \sqrt[5]{\frac{\rho V^5}{P n^2}} = \frac{J}{C_p^{1/5}}$$

where the effective thrust is the measured thrust of the propeller-body combination plus the drag of the body measured separately, and

P power absorbed by propeller, foot-pounds per second

V airspeed, feet per second

D propeller diameter, feet

n propeller rotational speed, revolutions per second

ρ mass density, slugs per cubic foot

These coefficients were plotted against V/nD . The results are given in the following figures:

Figure

- 6 - 9 characteristic curves for three-blade propeller in front hub
- 10 - 13 characteristic curves for four-blade propeller, single rotation
- 14 - 18 characteristic curves for four-blade propeller, dual rotation
- 19 - 22 characteristic curves for six-blade propeller, single rotation
- 23 - 27 characteristic curves for six-blade propeller, dual rotation
- 28 - 31 characteristic curves for eight-blade propeller, single rotation
- 32 - 36 characteristic curves for eight-blade propeller, dual rotation
- 37 - 39 effect of spinner length on efficiency
- 40 efficiency-envelope comparisons for different solidities
- 41 - 42 ratio of power absorbed per blade at peak efficiency to that of a three-blade propeller, single and dual rotation
- 43 - 47 comparisons of efficiency envelopes for tractor and pusher propellers
- 48 - 55 effect of dual rotation on efficiency and thrust at constant power
- 56 design chart for propellers 3155-6 and 3156-6 of different solidities, single rotation
- 57 design chart for propellers 3155-6 and 3156-6 of different solidities, dual rotation
- 58 relation between helical tip speed, forward speed, and equivalent V/nD

The results of the pusher tests are in general agreement with the tractor tests previously reported (references 1 and 2) as regards the effect of dual rotation on power absorbed and efficiency. These effects may be observed in detail from an inspection of the characteristic curves presented in figures 14 to 17, 23 to 26, and 32 to 35, wherein representative results from the single-rotation tests are superimposed on the dual-rotation plots. Of general interest is the magnitude of the gain in efficiency due to dual rotation, which was somewhat greater than experienced in the tractor investigation, and also the relative power absorbed by the single and dual propellers, which was about the same as for the tractor tests. The consequences of those effects are analyzed more fully in detail later.

Effect of mounting single-rotating propellers in tandem hubs.— The modal conditions for the single-rotation tests were identical to those for the dual-rotation tests in that the same hubs and spinners were used. In both cases half the total number of blades were in each hub of the tandem arrangement. As the single-rotation blades were arranged in this unorthodox manner, it was desired that the effect of mounting the blades all in a single hub should also be determined for the one case of four blades.

Figures 10 to 13 present the results of separate tests made with all four blades in the front hub, four blades in the rear hub, as well as two blades in each hub. The tests seem to confirm the theory that the set-up with two blades in each hub would result in an efficiency that is the average of efficiencies obtained with the four blades tested separately in each hub. The front spinner covers approximately $2\frac{1}{2}$ inches more of each blade shank than the rear spinner, which accounts for the appreciably higher efficiency of the propeller in the front position, an increase of 1 to 4 percent.

Effect of spinner length.— It was realized that for the pusher tests the shape and the size of the spinner might have an important effect on the results. Two spinners were therefore investigated, a short spinner that was standard for all tests, and a long one (see fig. 2) used for a few tests with six-blade single and dual propellers. The long spinner was so designed that it might either be fixed or allowed to rotate.

Comparisons of the relative merits of the long and the short spinners are made on the basis of a net efficiency; the drag of the body with the short spinner is used for the computations. This form of comparison is necessary because the long spinner added drag, which should be charged against the propeller if the only purpose of lengthening the spinner is to increase the propulsive efficiency.

A gain of 2 to 3 percent (see figs. 37 to 39) in net efficiency was realized for the long spinner over the short spinner for single rotation; the effect on efficiency of having the spinner rotating or fixed was negligible.

The small gain in net efficiency for the long spinner was confined to the low V/nD range for the dual-rotating propellers. That the long spinner benefited the single-rotating propellers to a greater extent than the dual propellers may be accounted for by the fact that the rotating slipstream of the single propellers might have caused early separation from the short spinner. This rotating slipstream was not present for dual rotation.

Inasmuch as the long spinner added drag, a loss in efficiency might be expected for dual rotation. That this loss was not realized was probably due to the fact that the long spinner was also larger in diameter than the small one and thus covered up more of the poor blade shanks.

Effect of solidity.-- Envelope efficiency comparisons for propellers of different solidity are not of much practical interest because the power absorption is different for different solidities. Curves of this type provide a measure of blade efficiency, or the effect of blade interference. The general effect of increasing the solidity for single rotation, shown in figure 40(a), was to reduce the efficiency several percent over the V/nD range; a drop of 4 to 10 percent was experienced in going from three to eight blades. The loss in efficiency resulting from increasing the solidity appeared to be negligible for dual rotation, as may be noted from figure 40(b).

Comparisons are made in figures 41 and 42 for the power absorbed at peak efficiency per blade, relative to that for the blades of a three-blade propeller. These plots indicate that the effectiveness of each blade of a dual propeller in absorbing power was substantially more

than that for a single-rotating propeller, an effect noticed for the tractor propellers as well (reference 2). The individual blades of an eight-blade dual propeller absorbed approximately 84 percent as much power as each blade of a three-blade single propeller as compared with 81 percent for an eight-blade single propeller.

Comparisons of single and dual rotation for both tractor and pusher positions.—The improvement in efficiency due to dual rotation was more pronounced for the pusher propellers (fig. 43) than for the tractor propellers of references 1 and 2. The gain for the pusher propellers ranged from 1 to 16 percent as compared with 1 to 8 percent for the tractor propellers, depending upon the V/nD , the number of blades, and similar factors.

The greater improvement in efficiency due to dual rotation for the pusher position was not generally due to an increased efficiency of the dual combination but rather to a greatly reduced efficiency of the single-rotating propellers. It appears from figure 43 that the efficiency of the dual propellers remained about constant for both positions but that the single-rotating propellers were less efficient for the pusher position because of the probable effect of the rotating slipstream and spinner on inducing early separation.

More detailed comparisons of tractor and pusher propellers are given in figures 44 to 47. The single-rotating pusher propellers were from 0 to 7 percent less efficient than the corresponding tractor propellers and from 0 to 10 percent less efficient than the tractor propellers tested with the wing. The dual propellers provided about the same efficiency, within a few percent, irrespective of whether they were tested as tractors or as pushers and whether or not a wing was present.

Comparisons of efficiency and thrust based on constant power.—Since the dual-rotating propellers absorbed somewhat more power at the same blade-angle setting than the single-rotating propellers, the effect of dual rotation on efficiency and thrust should be based on equal power absorption. Such comparisons are made in figures 48 to 50 for efficiency and in figures 51 to 53 for thrust.

The efficiency gains at peak η due to dual rotation compare favorably with those based on the V/nD envelope curves; even greater gains are evident, however, for con-

ditions corresponding to the take-off and climb. This fact is brought out to better advantage in figures 51 to 53, wherein the relative thrust of dual- and single-rotating propellers is plotted. It may be noted that the take-off and climbing thrust was increased as much as 40 or 50 percent for the most extreme case, namely, the four-blade propeller operating at $C_p = 0.6$.

This increased thrust may be accounted for partly by the fact that dual-rotating propellers absorbed more power than single-rotating ones and, consequently, the blade-angle settings for the dual propellers were lower than for single-rotating propellers, particularly for the take-off and climbing conditions. This lower blade-angle setting resulted in greater thrust for a given power output, owing to the higher lift-drag ratios of the elements and to more favorable velocity-vector relationships. Also, with dual propellers the losses due to slipstream rotation are greatly reduced, which accounts for a large percentage of the gain in efficiency.

That the dual-rotating propellers absorbed more power than the single-rotating propellers, particularly for the take-off and climbing conditions, may be accounted for, as mentioned in previous reports, by the fact that the rear propeller of the dual arrangement was operating in the slipstream of the front propeller which was twisting in a direction opposite to the rotation of the rear propeller. This condition indicates that the rotational velocity of the rear propeller relative to the air was greater than that of the front propeller of the dual combination; hence, the rear propeller was producing more thrust. The reverse effect was present for the single-rotating propellers and accounts for the large differences in power absorbed for single- and dual-rotating propellers.

That the rear propeller of the dual combination had a higher effective rotational velocity than the front one will probably result in higher compressibility losses when the propellers are operated at high tip speeds, although the differences may be unimportant for the high-speed flight condition.

Of interest, also, is the effect of solidity on efficiency at constant power, which is shown in figures 54 and 55. It may be noted that increasing the solidity greatly increased the efficiency for the take-off and climbing conditions, with some loss at high speed. This

effect of increased efficiency at low values of V/nD , discussed in some detail in reference 3, was due chiefly to reducing the angle of attack of operation, thereby increasing the L/D of the sections.

Preliminary design charts.— In the selection of propellers for new high-performance airplanes there may be some choice as to the number of blades to be employed and also whether they should be single or dual rotating. In order to save time in selecting propellers, several charts are included that may prove to be convenient.

Figures 56 and 57 present composite skeleton C_s charts that show the envelopes of the operating curves for three-, four-, six-, and eight-blade single- and dual-rotating propellers. The relative efficiencies and diameters may be determined directly for any set of conditions.

Inasmuch as compressibility is an important design parameter, which is neglected in the C_s charts, an additional chart is provided in figure 58 to relate rotational and helical tip speeds with V/nD . The speed of sound in standard atmosphere is also given for convenience. With forward speed and limiting helical tip speed known or assumed, the limiting V/nD and rotational speed may be read directly and used in connection with the C_s charts previously described. These charts thus provide an easy means for determining for preliminary computations not only the diameter but also the gear ratio for peak-efficiency operation for each propeller solidity.

CONCLUSIONS

The general effects of dual rotation on propeller characteristics found in this investigation of pusher propellers differed only in degree from those listed in previous reports of tractor propellers. These effects are summarized more specifically in the following conclusions relating to the present investigation.

1. Single-rotating pusher propellers were found to be from 0 to 10 percent less efficient than corresponding tractor propellers; but dual-rotating pusher propellers had about the same efficiency as the corresponding tractor propellers.

2. The peak efficiency of dual-rotating pusher propellers was found to be from 1 to 16 percent higher than that for single-rotating propellers. The gain in efficiency depended upon the blade-angle setting and the number of blades, the higher of either the greater the gain.

3. Dual-rotating propellers were found to be substantially more efficient for the take-off and climbing conditions of flight than the single-rotating propellers, particularly for operation at high power coefficients.

4. The peak blade efficiency was found to decrease with increased number of blades for the single-rotating pusher propellers but not for the dual-rotating propellers.

5. The efficiency for the take-off and climbing conditions increased substantially with increases in number of blades for constant power input with a slight loss at the high-speed condition.

6. Dual-rotating propellers were found to absorb substantially more power at peak efficiency than single-rotating propellers of the same solidity; the effect was even more pronounced for the take-off and climb conditions.

7. The power absorbed per blade at peak efficiency decreased slightly with increased numbers of blades, more so for single rotation than for dual rotation.

8. A large increase in the length of the spinner resulted in several percent increase in the net efficiency of a single-rotating propeller but the gain was negligible for a dual-rotating propeller.

Langley Memorial Aeronomical Laboratory,
National Advisory Committee for Aeronautics,
Langley Field, Va.

REFERENCES

1. Biermann, David, and Hartman, Edwin P.: Wind-Tunnel Tests of Four- and Six-Blade, Single- and Dual-Rotating Tractor Propellers. NACA Rep. No. 747, 1942.
2. Biermann, David, and Gray, W. H.: Wind-Tunnel Tests of Eight-Blade Single- and Dual-Rotating Propellers in the Tractor Position. NACA ARR, Nov. 1941.
3. Biermann, David, and Conway, Robert N.: The Selection of Propellers for High Thrust at Low Airspeed. NACA ARR Oct. 1941.

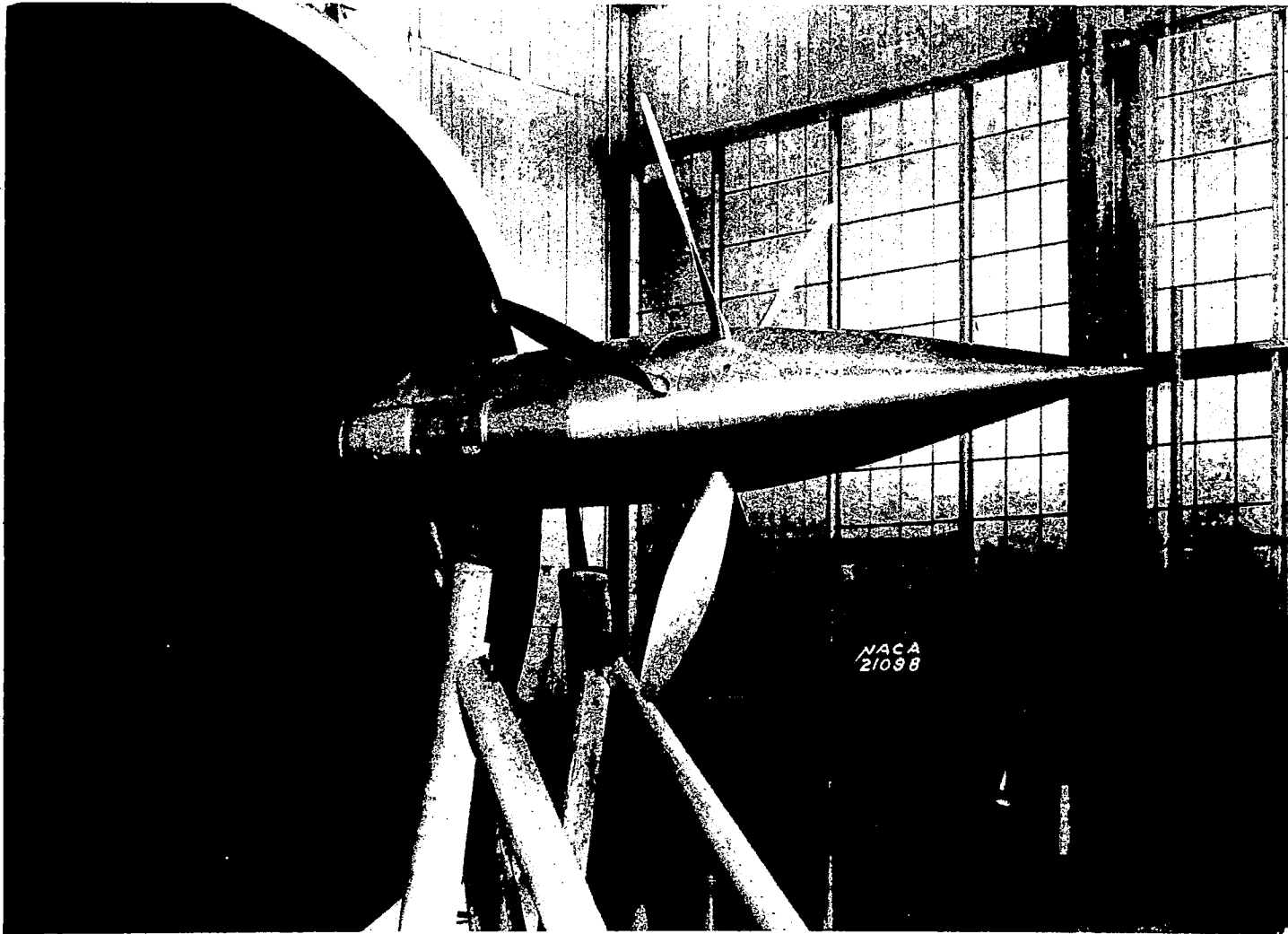


Figure 1.- Six-blade single-rotation propeller installed in long spinner.

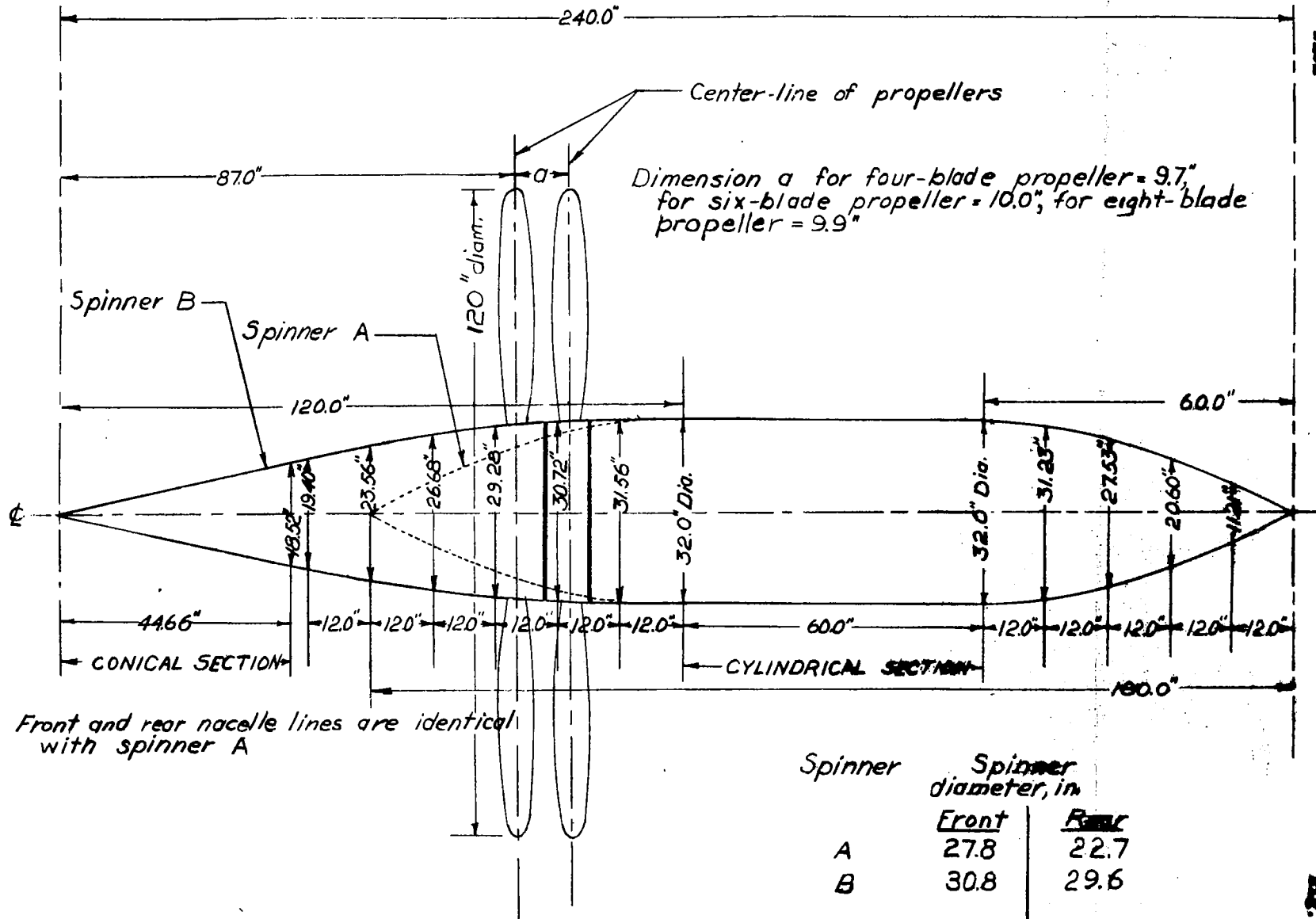


Figure 2.-Plan view showing dimensional details of nacelle.

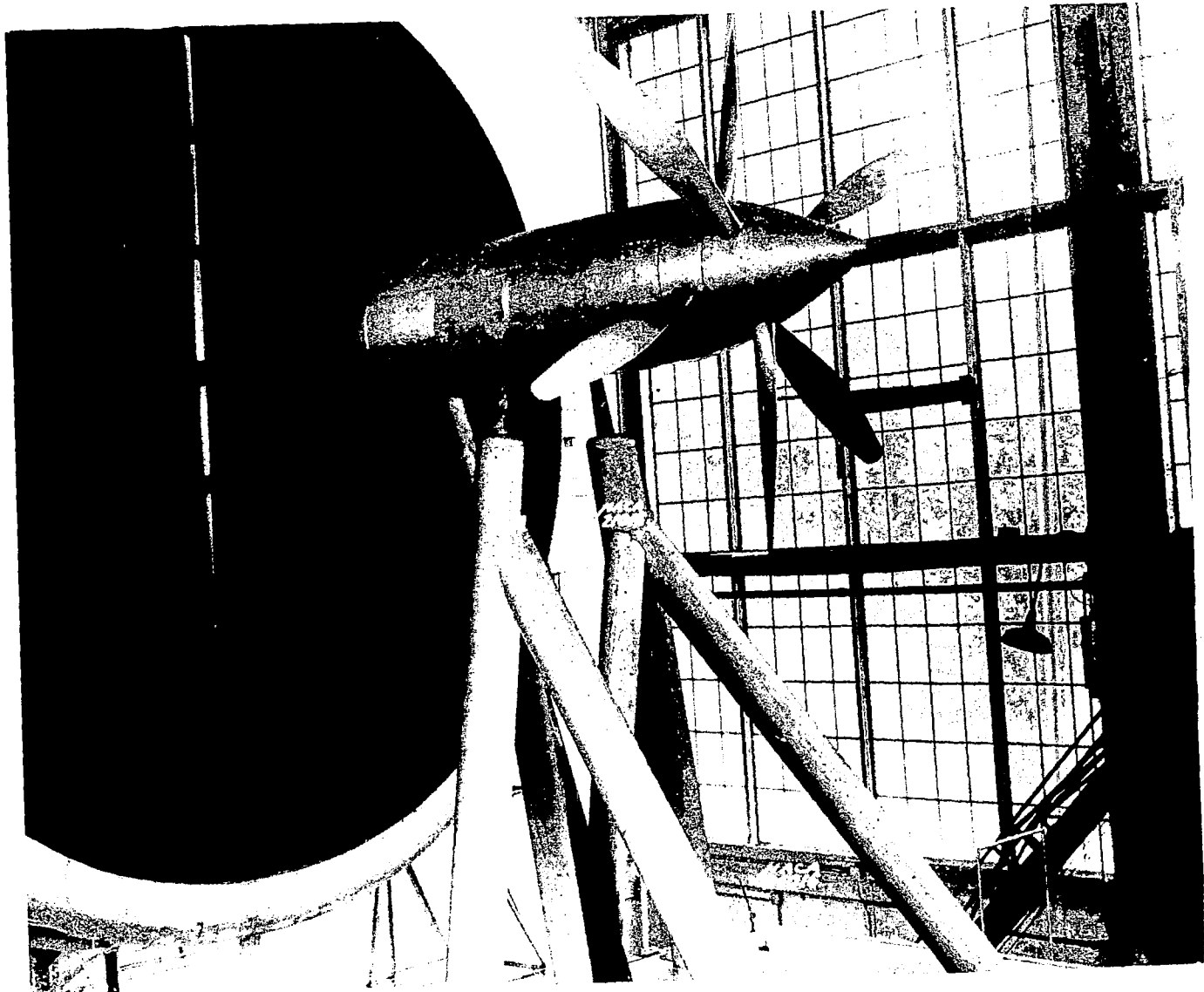


Figure 3.- Six-blade dual-rotation propeller installed in short spinner.

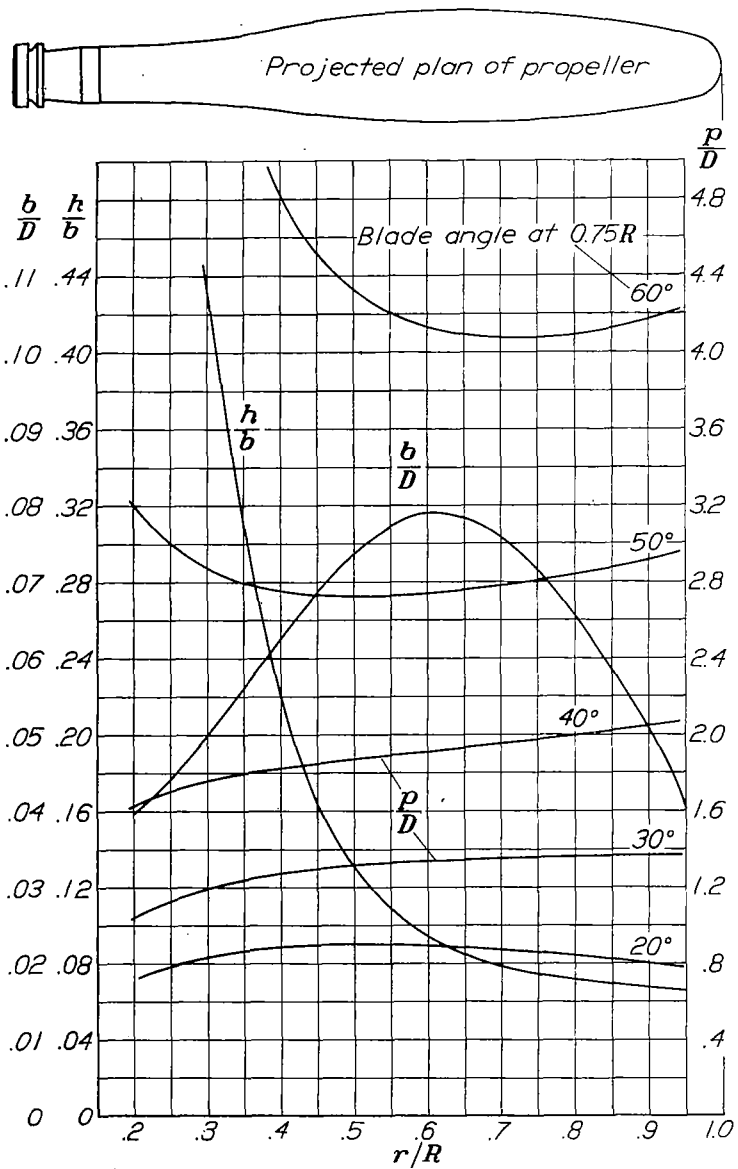


Figure 4.- Plan-form and blade-form curves for propellers 3155-6 and 3156-6. D, diameter; R, radius to the tip; r, station radius; b, section chord; h, section thickness; p, geometric pitch.

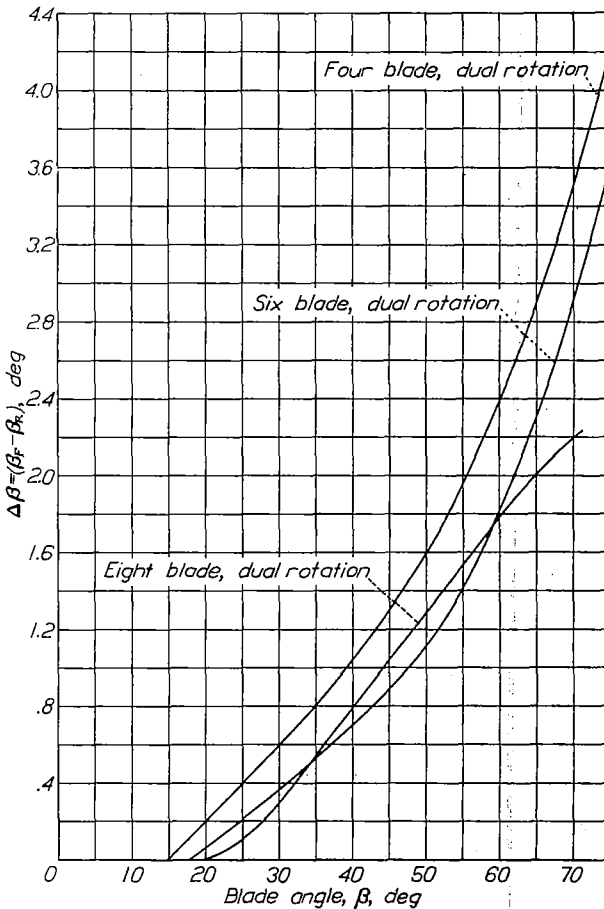


Figure 5.- Difference in blade angle of 0.75R for equal torque at peak efficiency.

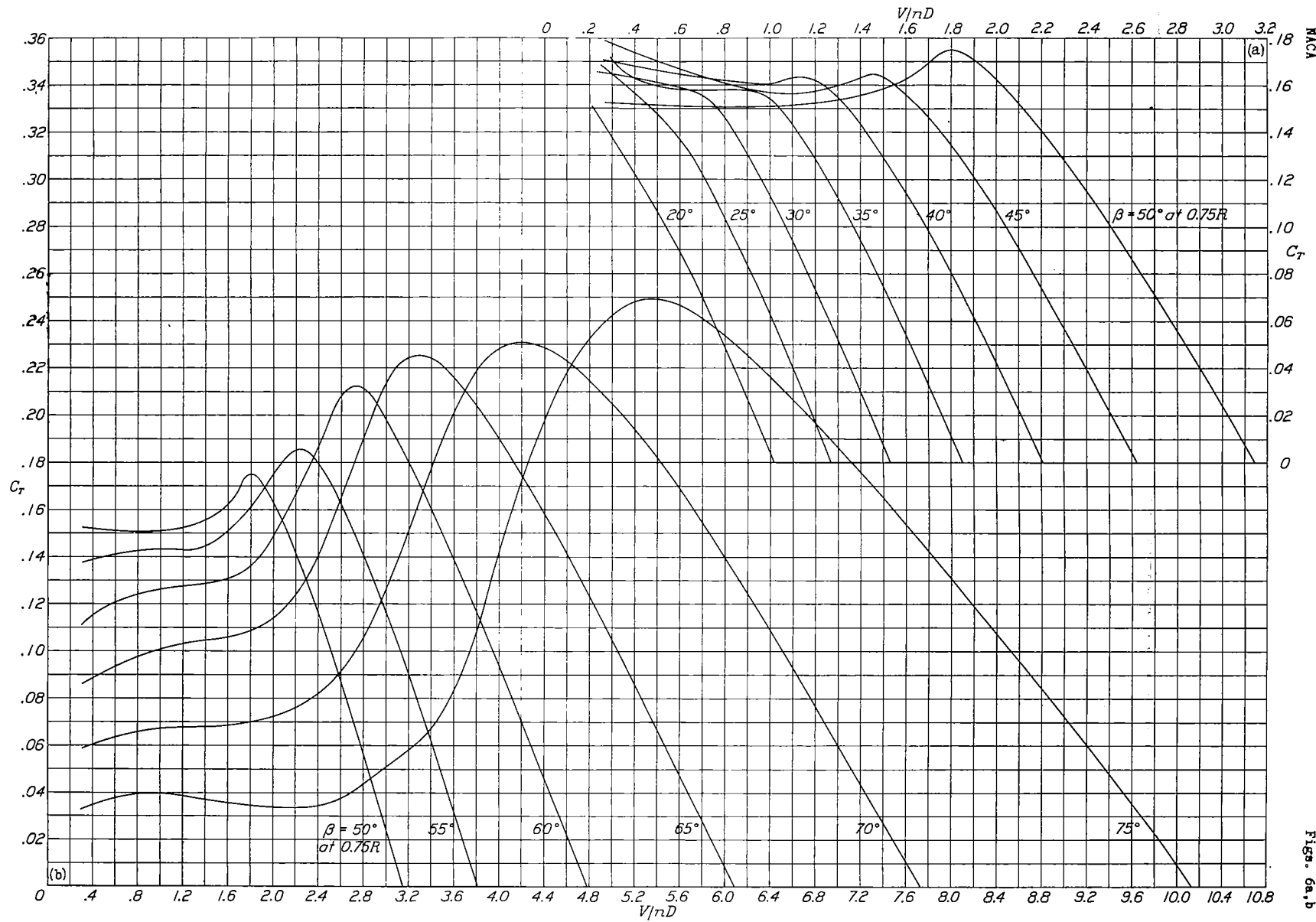


Figure 6(a,b).-Thrust-coefficient curves for three-blade single-rotation propeller on front hub.

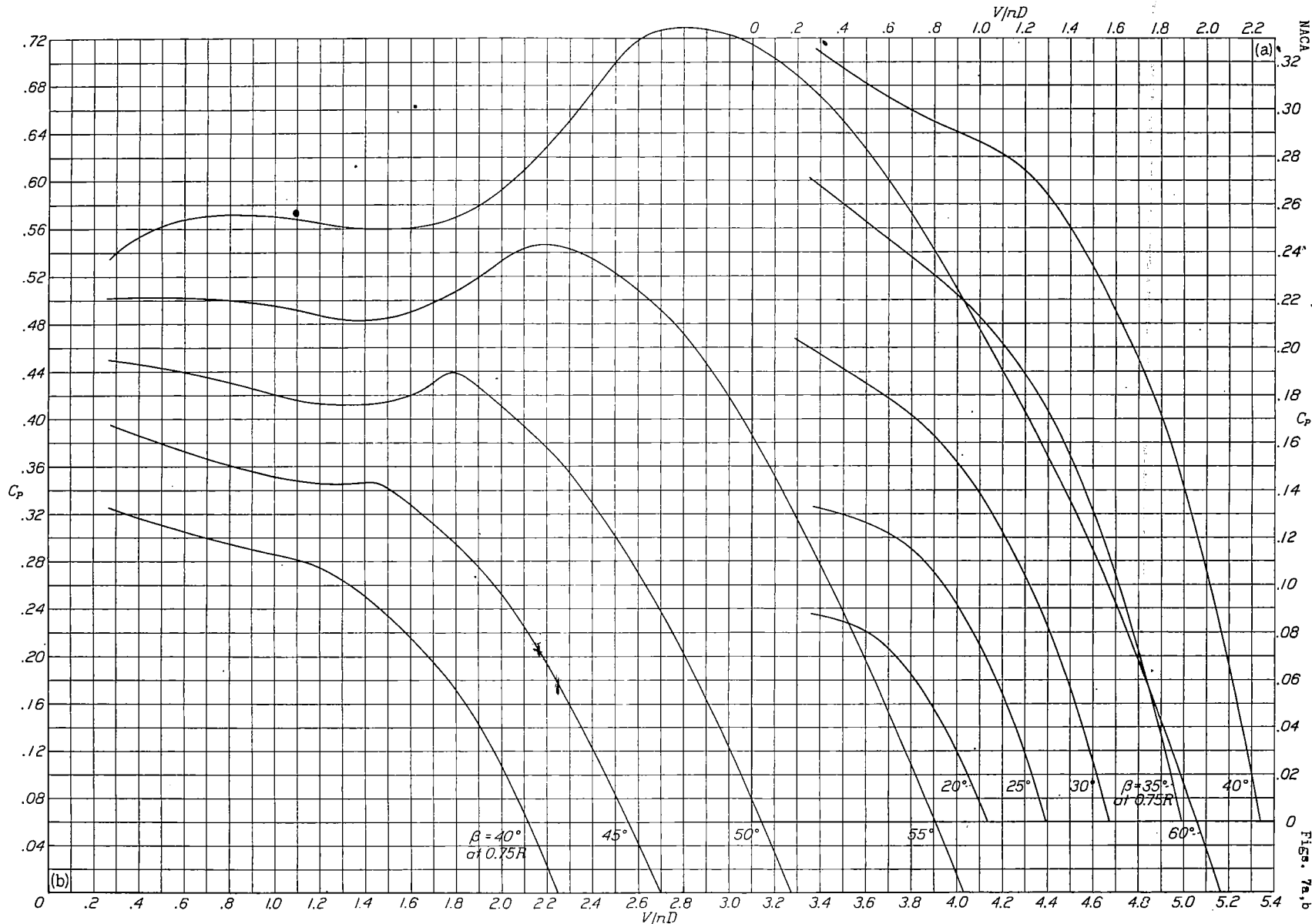


Figure 7(a,b).-Power-coefficient curves for three-blade single-rotation propeller, on front hub.

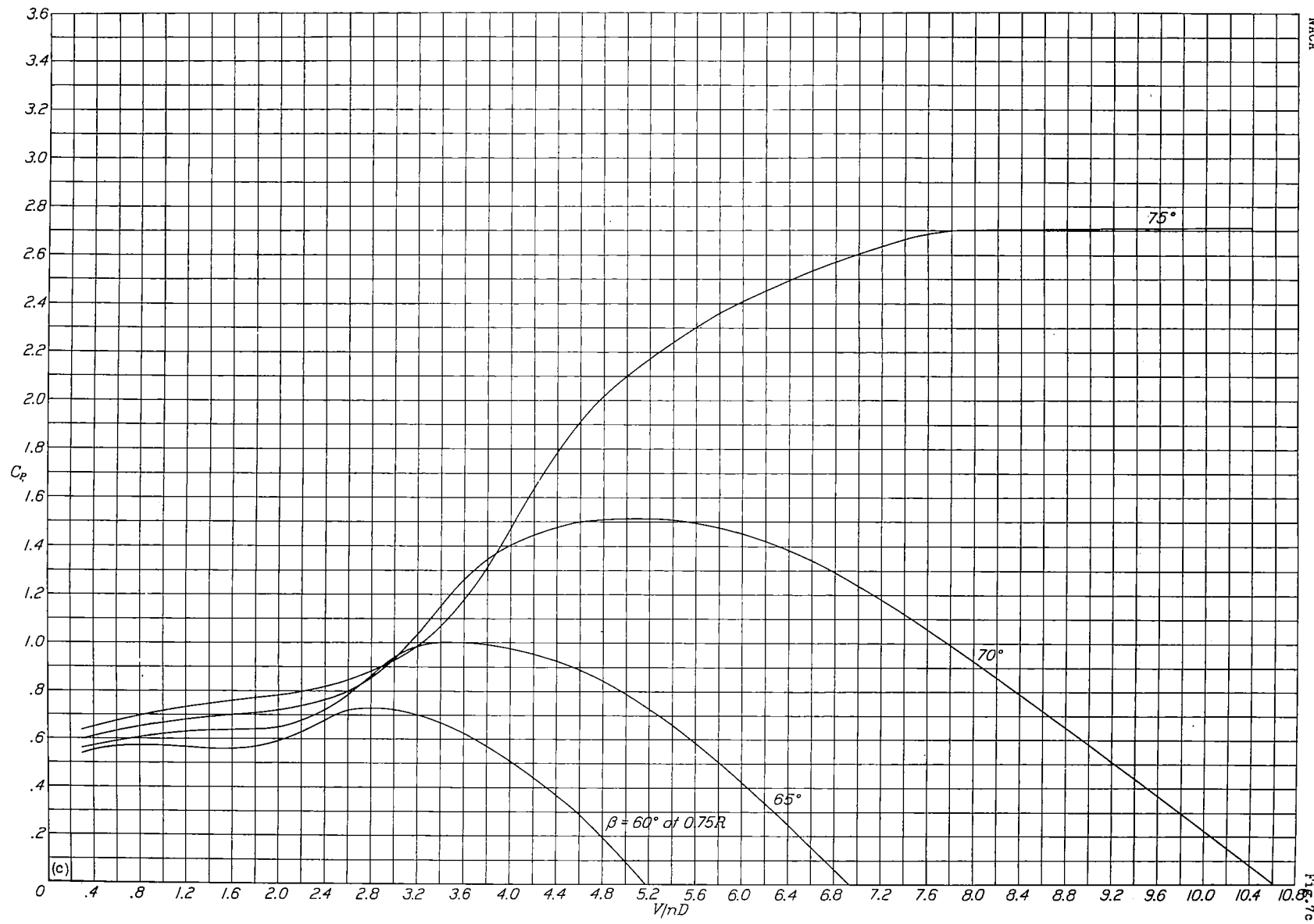


Figure 7(c).-Power-coefficient curves for three-blade single-rotation propeller on front hub.

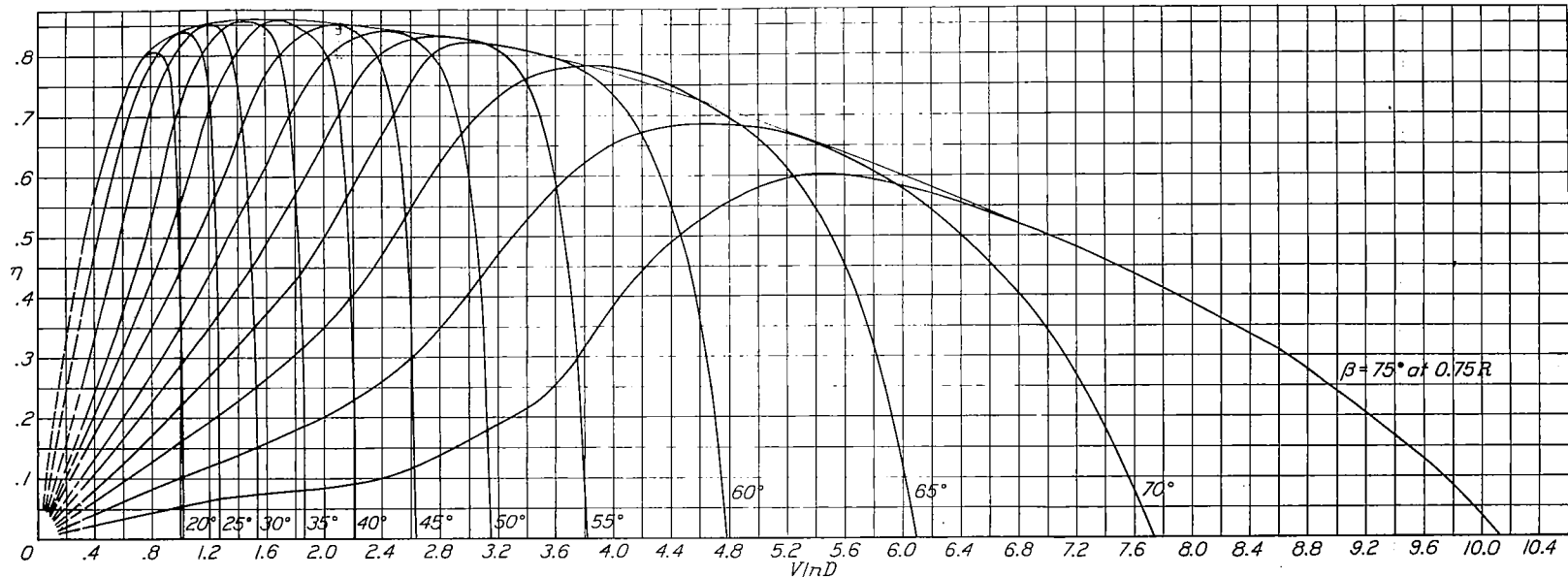


Figure 8.-Efficiency curves for three-blade single-rotation propeller, on front hub.

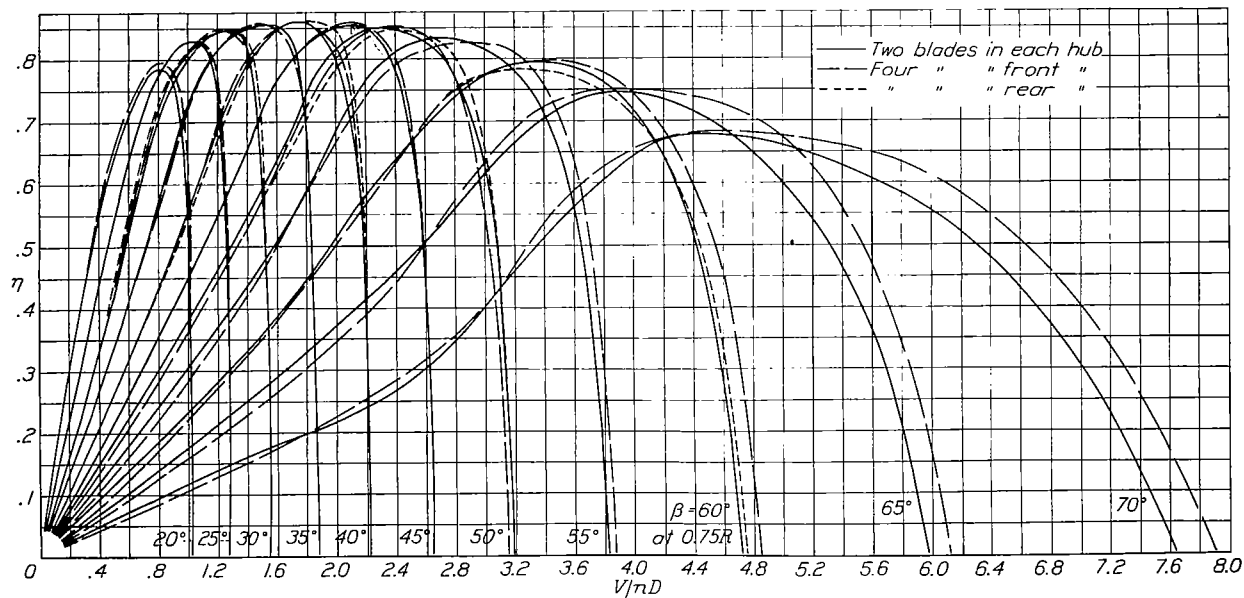


Figure 12.-Efficiency curves for four-blade single-rotation propeller.

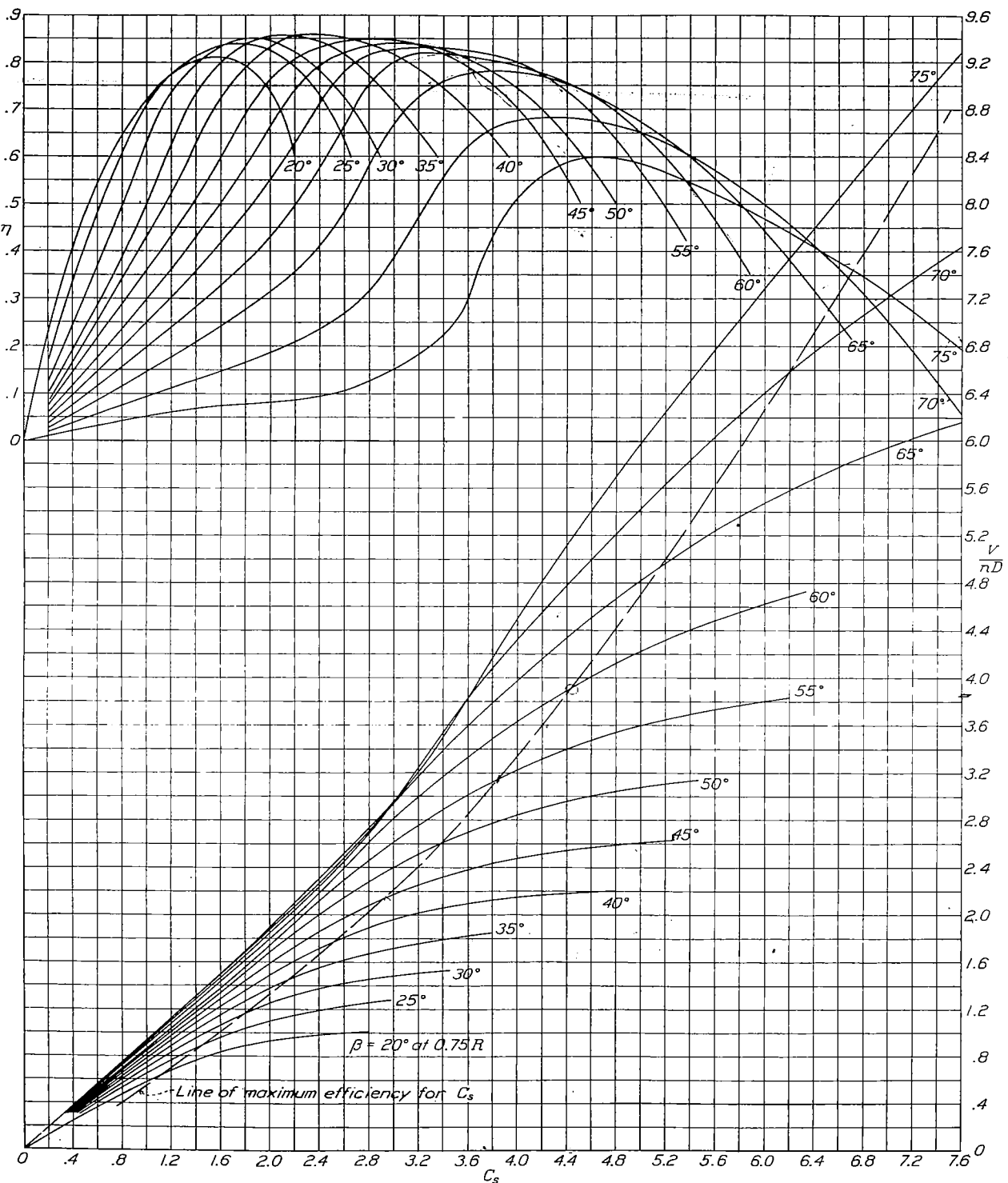


Figure 9.-Design chart for propeller 3155-6, three-blade single rotation.

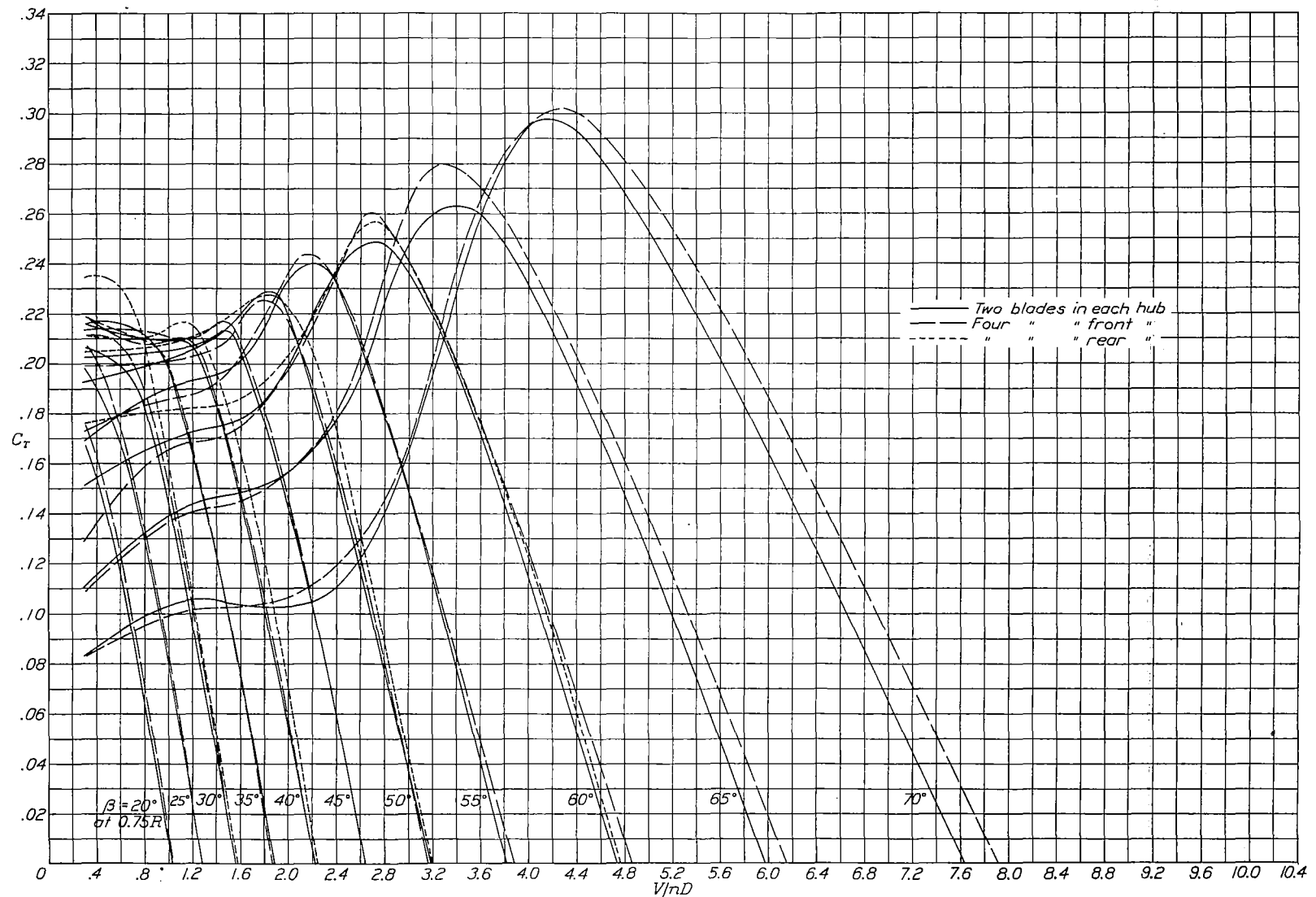


Figure 10.-Thrust-coefficient curves for four-blade single-rotation propeller.

FIG. 10

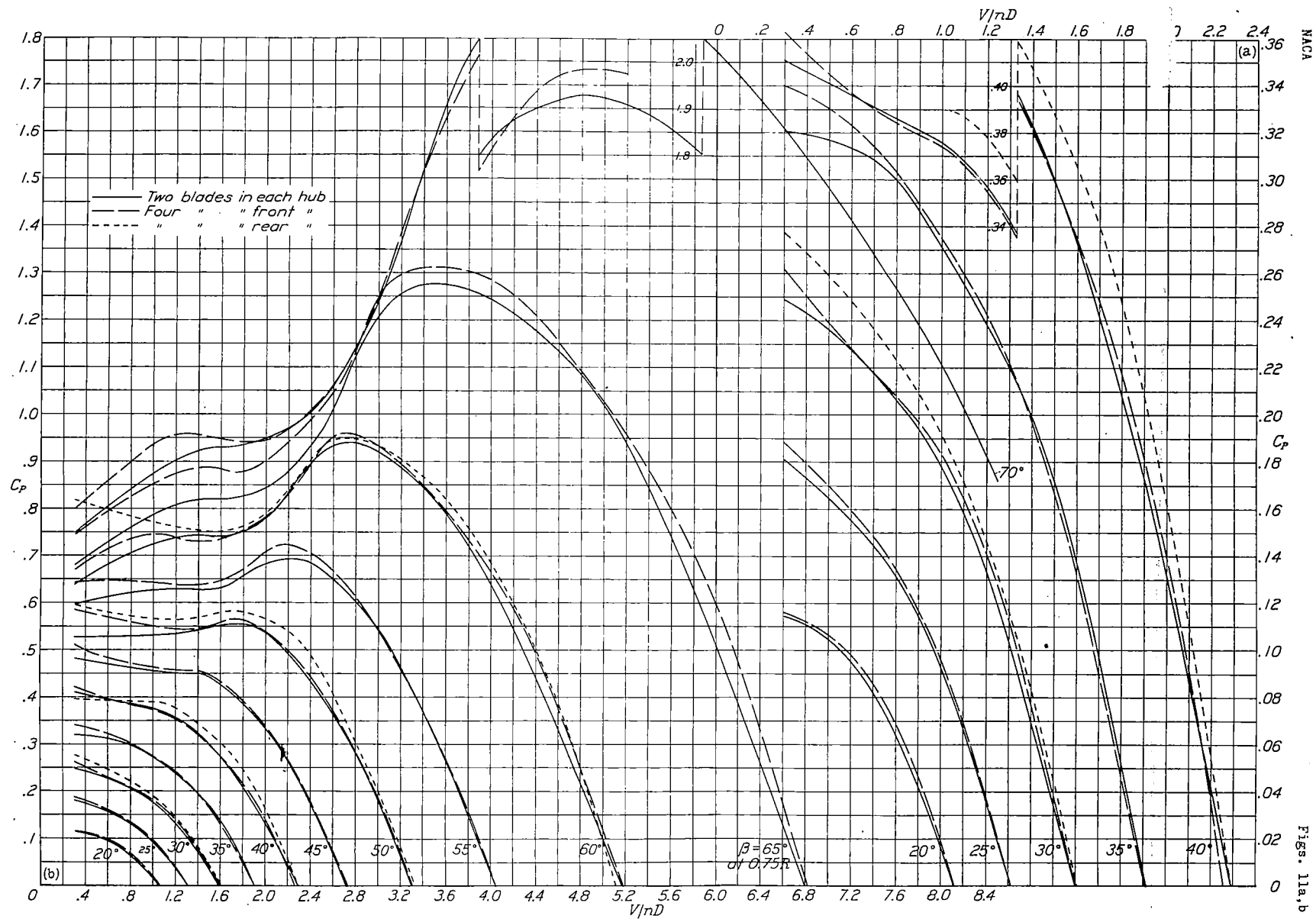


Figure 11(a,b). - Power-coefficient curves for four-blade single-rotation propeller.

Fig. 13

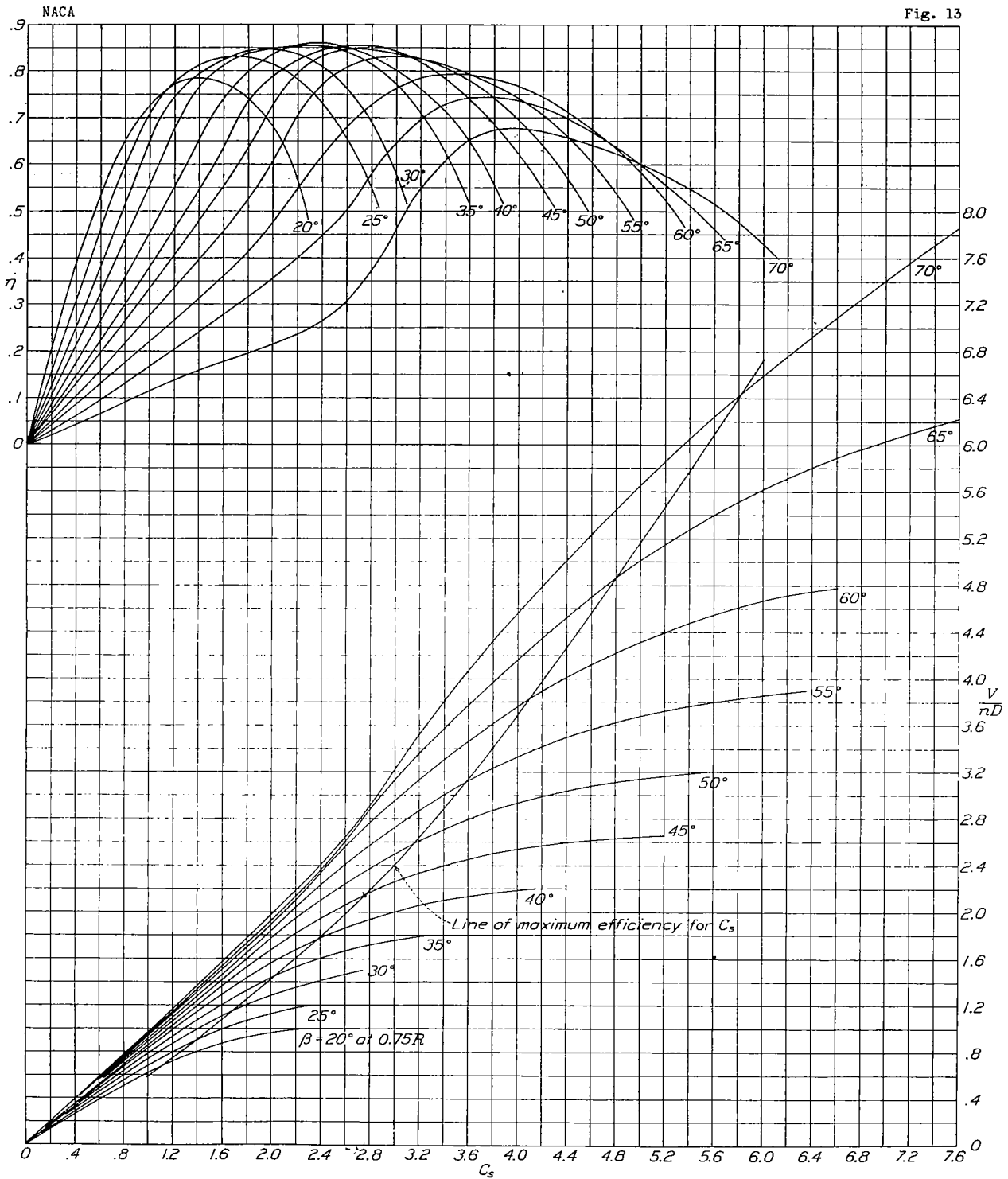


Figure 13.-Design chart for pusher propeller 3155-6 four-blade single-rotation.

45° $\beta = 2, 15$

$C_s = 2.75$

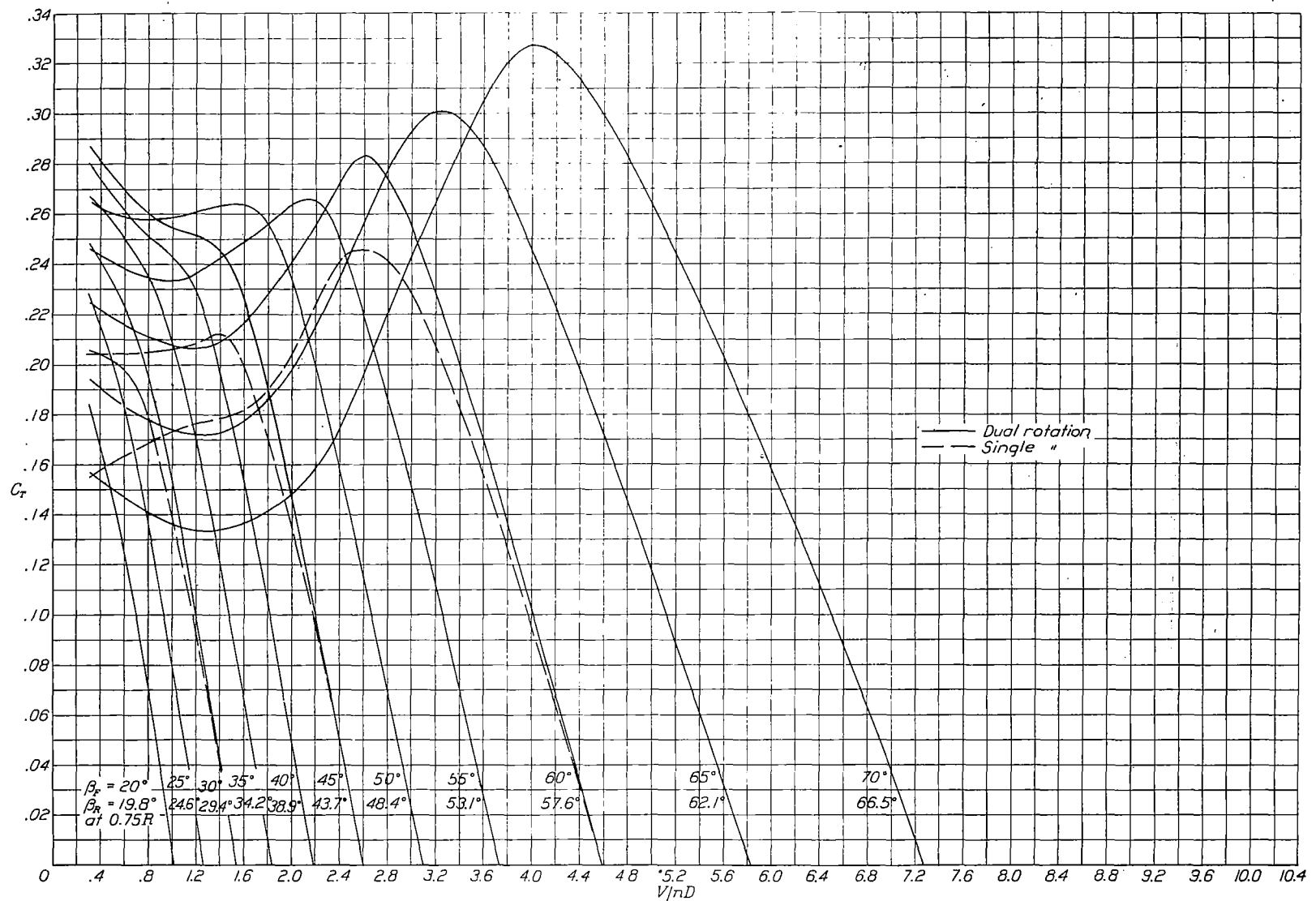


Figure 14.-Thrust-coefficient curves for four-blade dual-rotation propeller, showing superimposed curves for 30°, 45°, and 60°, single rotation.

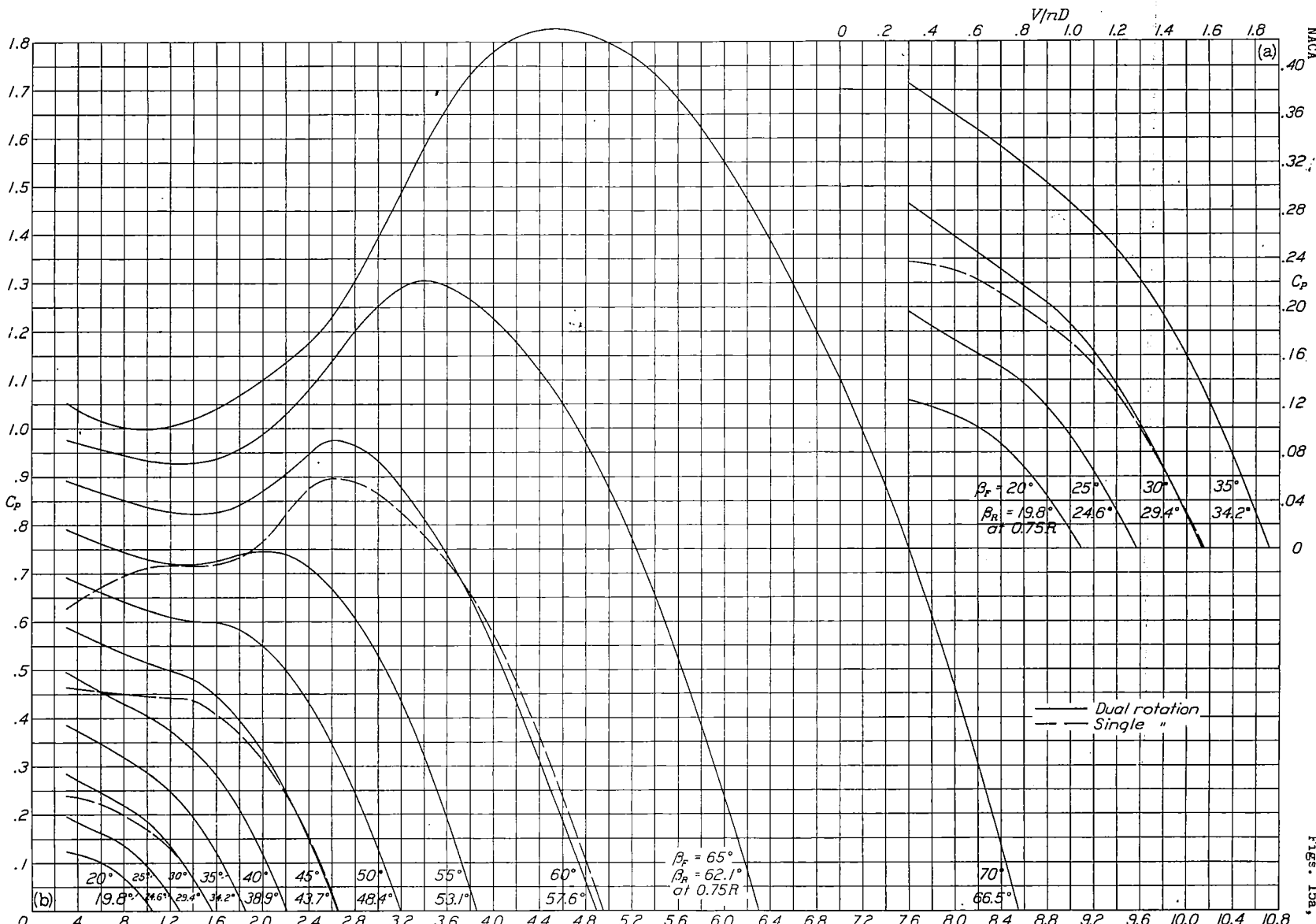


Figure 15(a,b)-Power-coefficient curves for four-blade dual-rotation propeller.

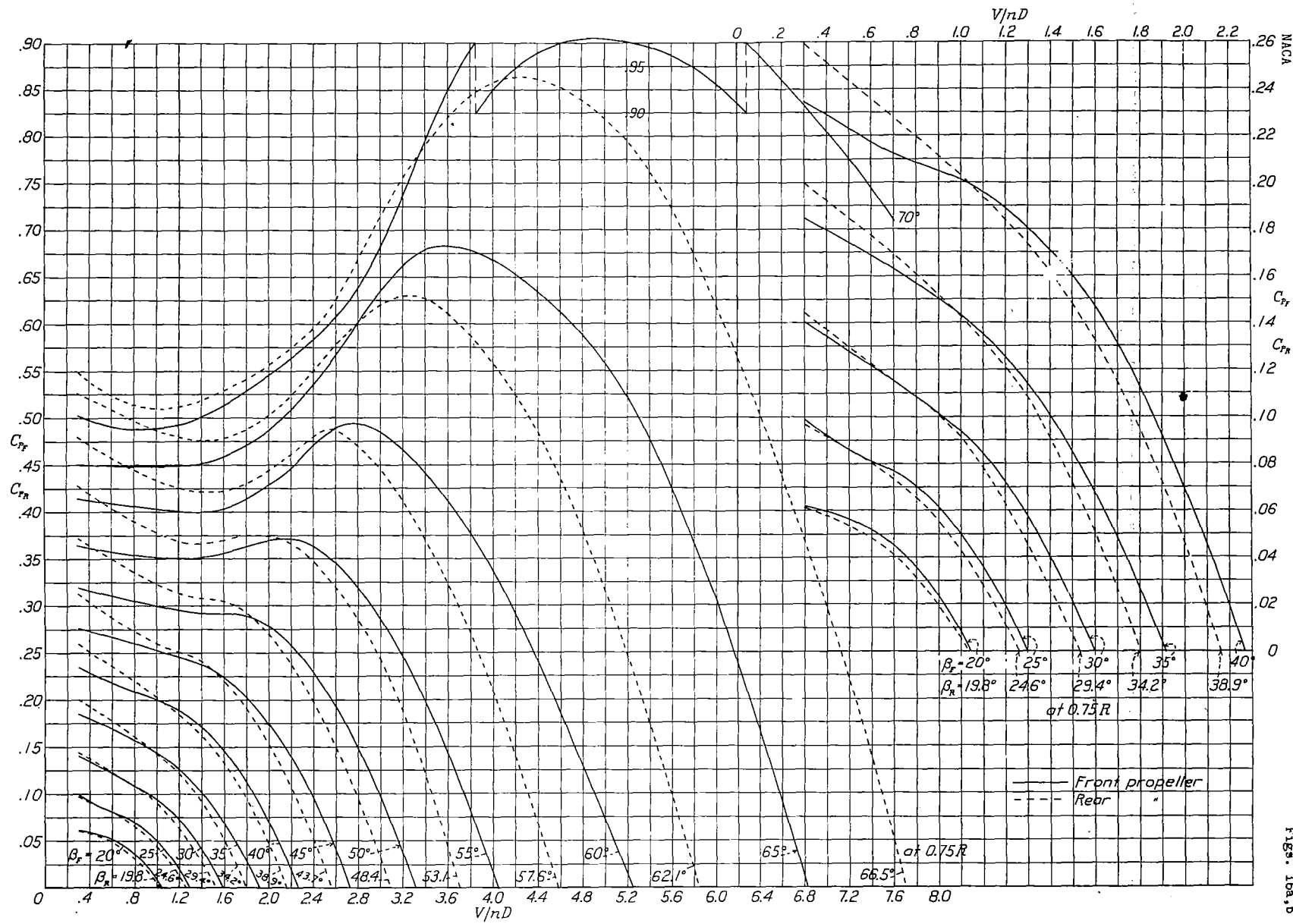


Figure 16(a,b).-Individual power-coefficient curves for four-blade dual-rotation propeller.

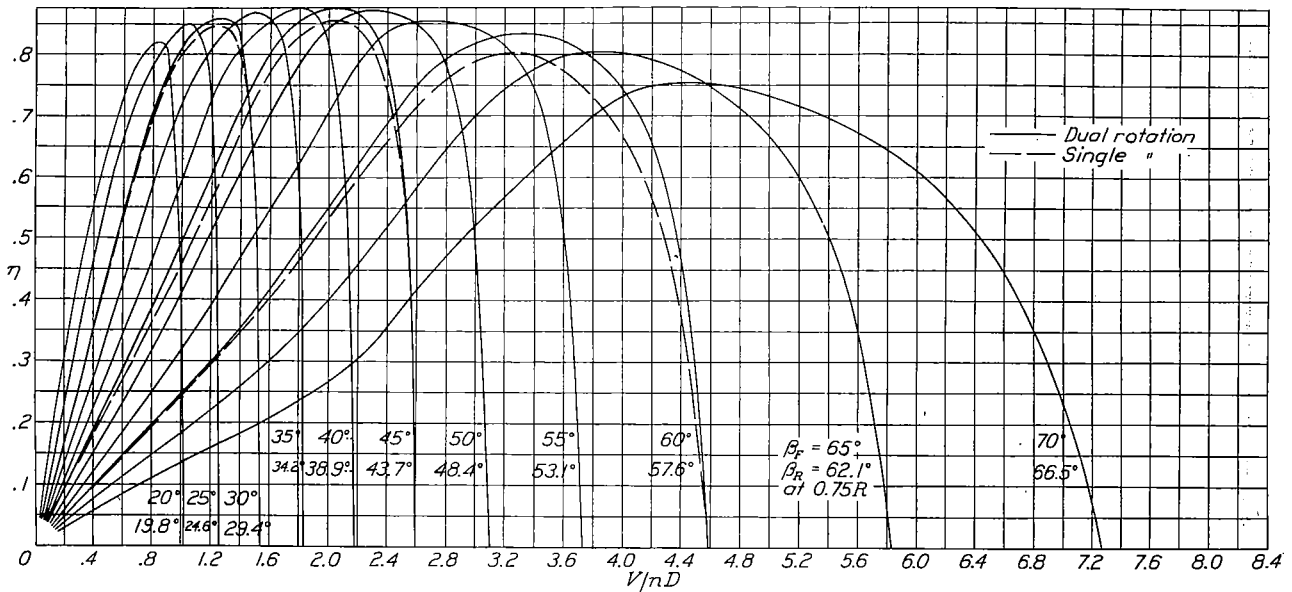


Figure 17.-Efficiency curves for four-blade dual-rotation propeller showing superimposed curves for $30^\circ, 45^\circ$, and 60° single rotation.

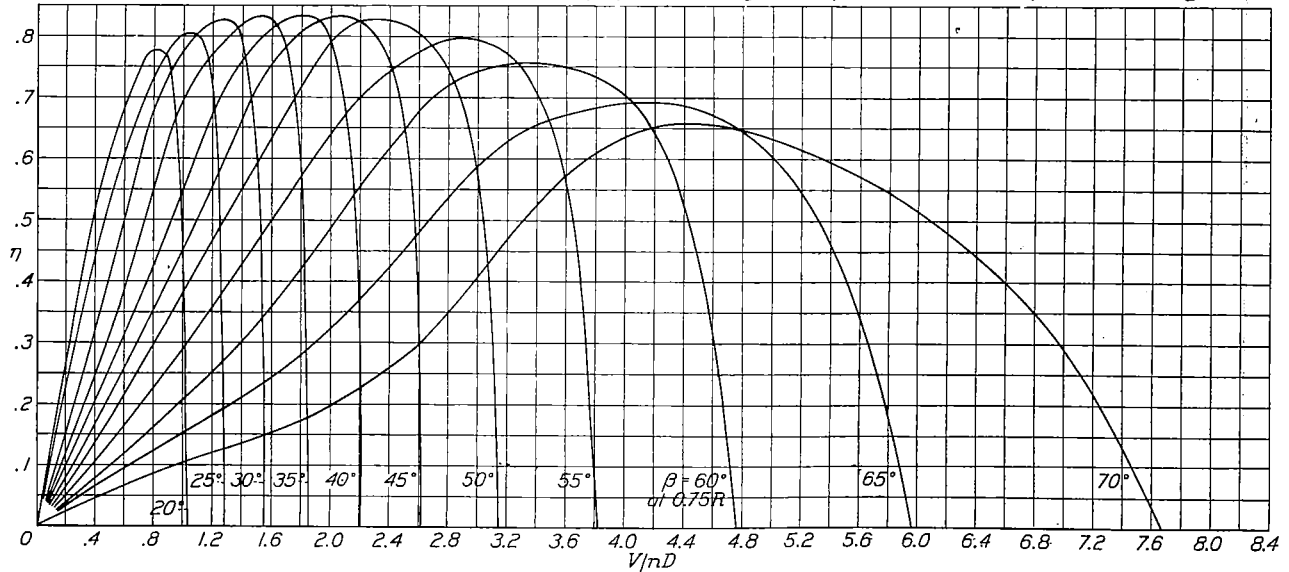


Figure 21.-Efficiency curves for six-blade single-rotation propeller.

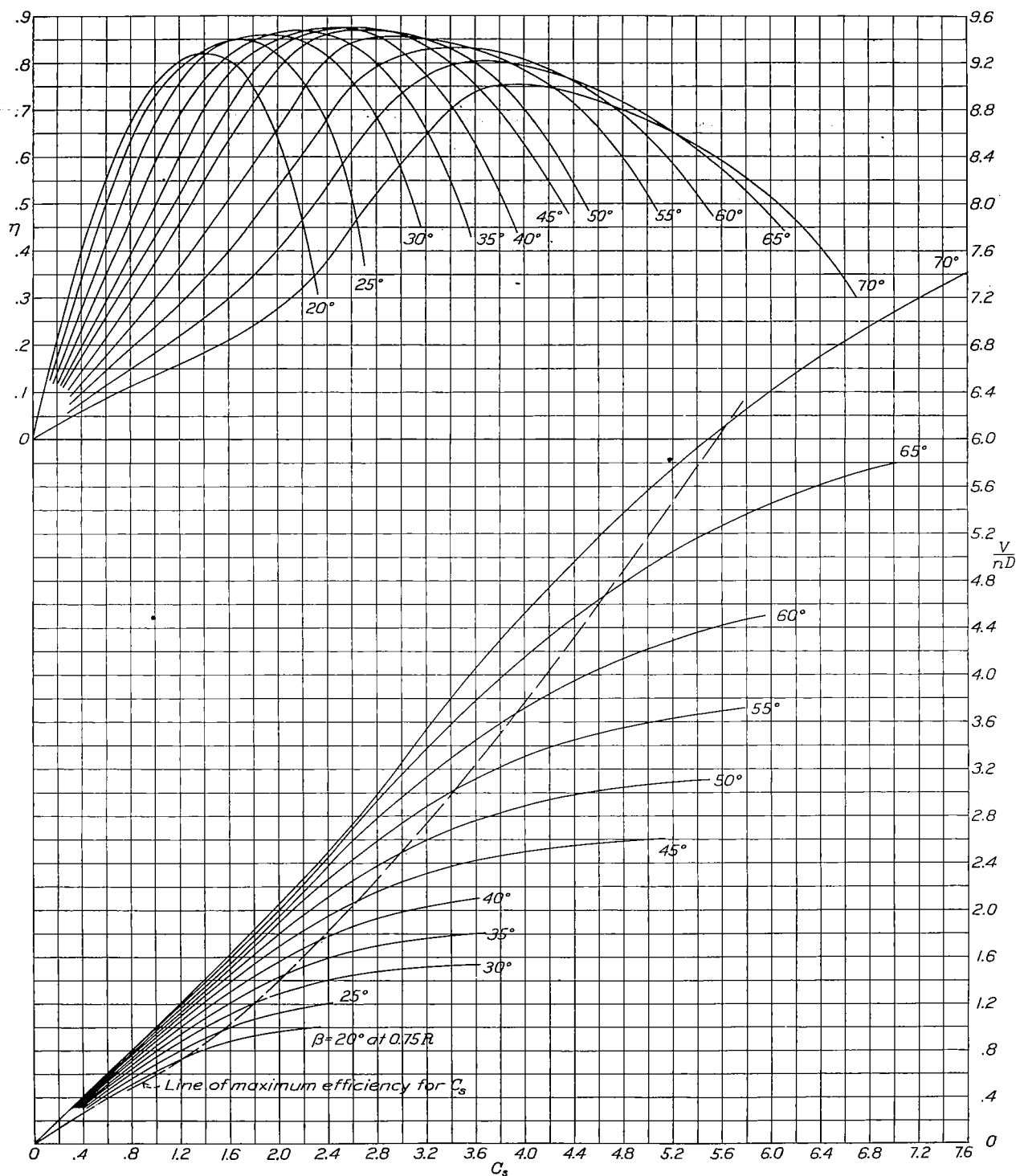


Figure 18.-Design chart for propellers 3155-6(R.H.) and 3156-6(L.H.), four-blade dual-rotation propeller.

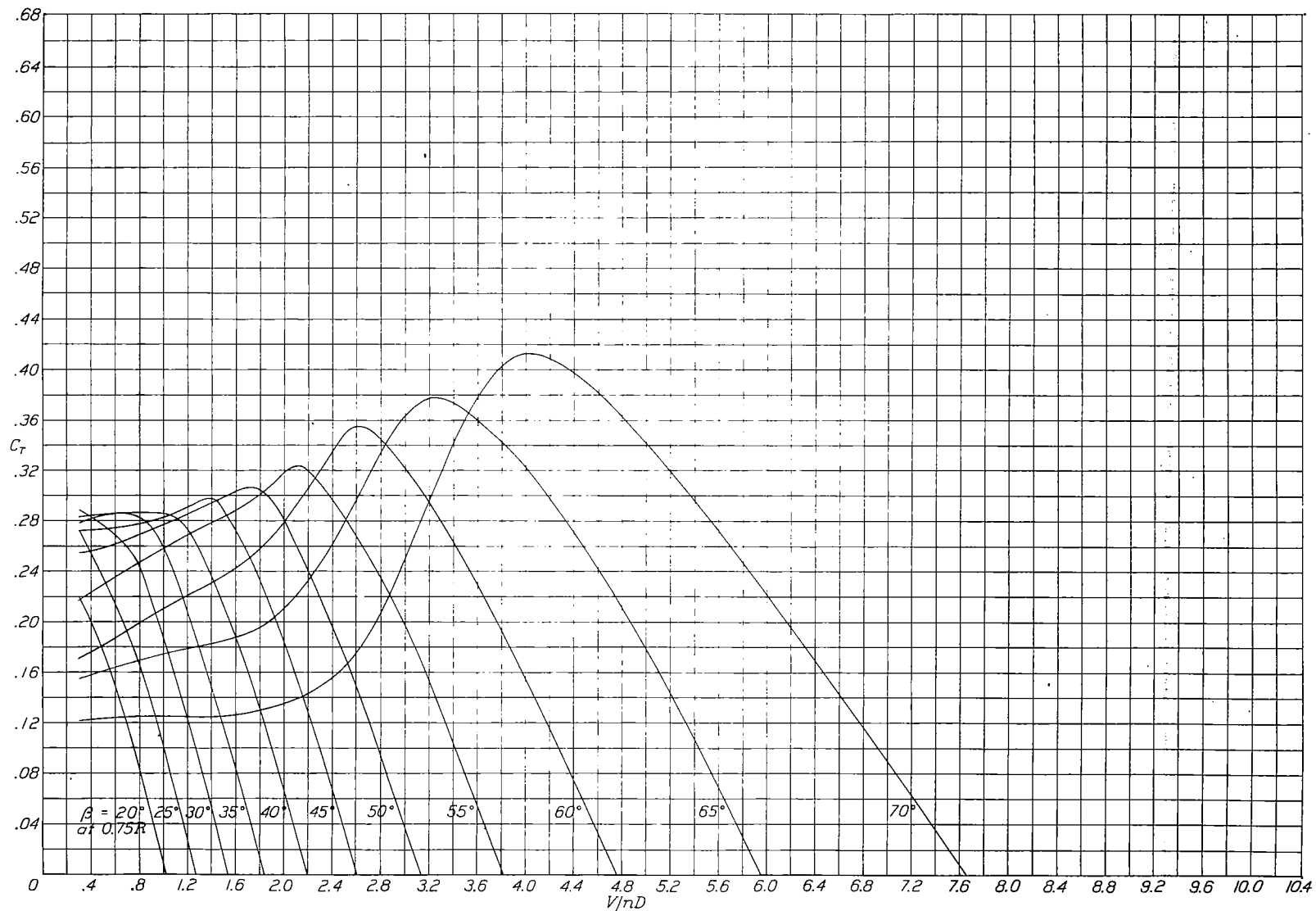


Figure 19.-Thrust-coefficient for six-blade single-rotation propeller.

FIG. 19

NACA

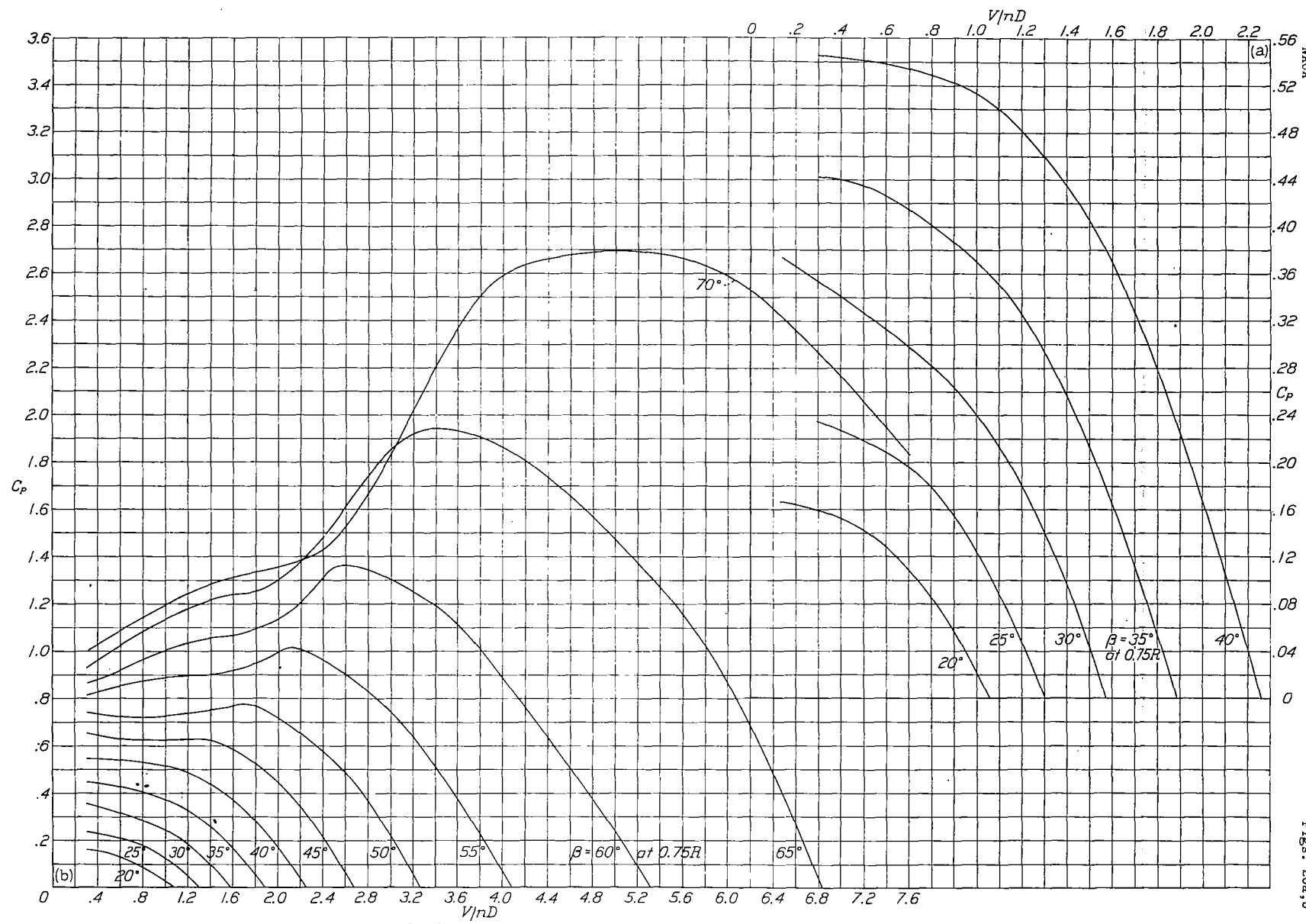


Figure 20(a,b).-Power-coefficient curves for six-blade single-rotation propeller.

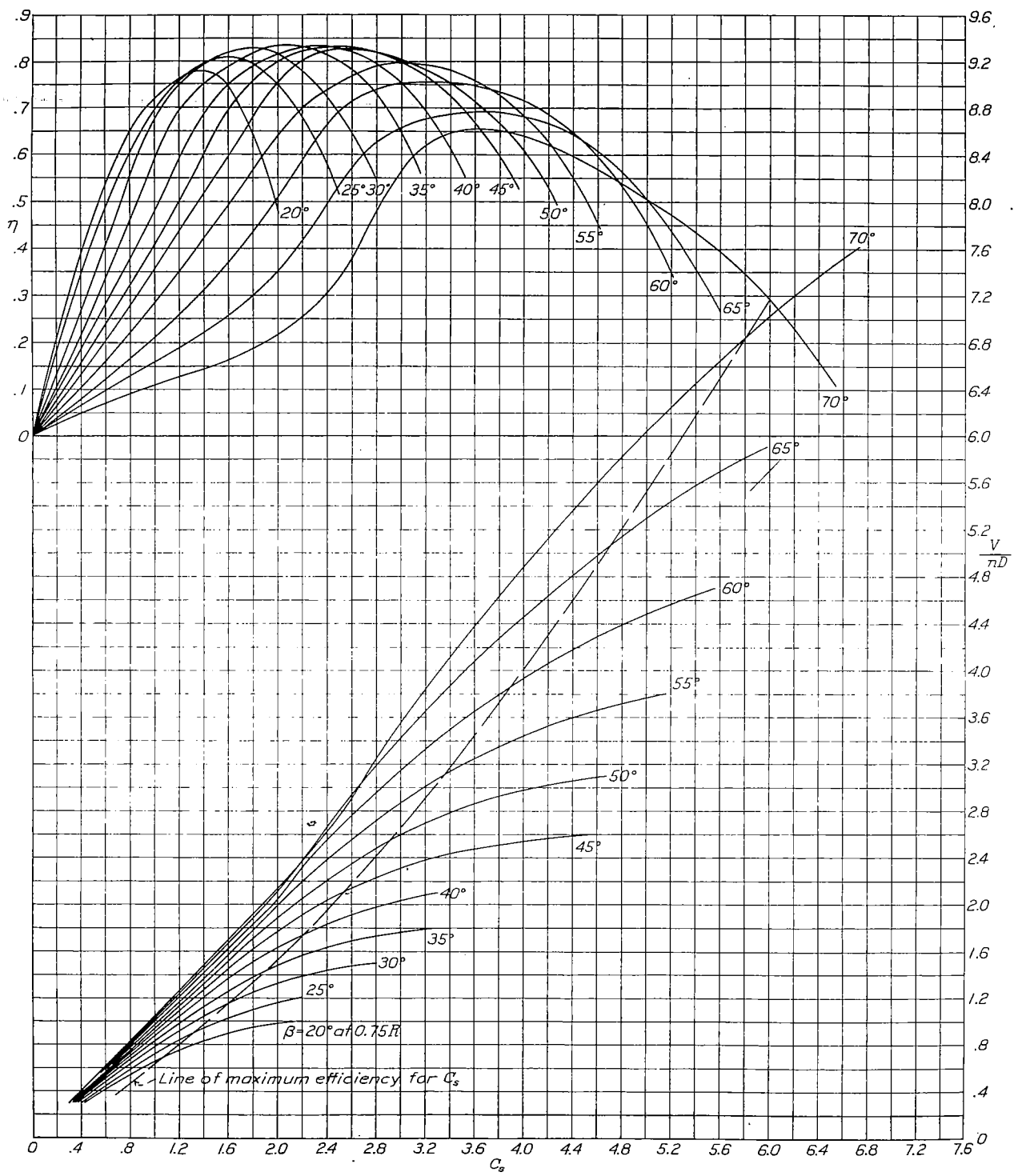
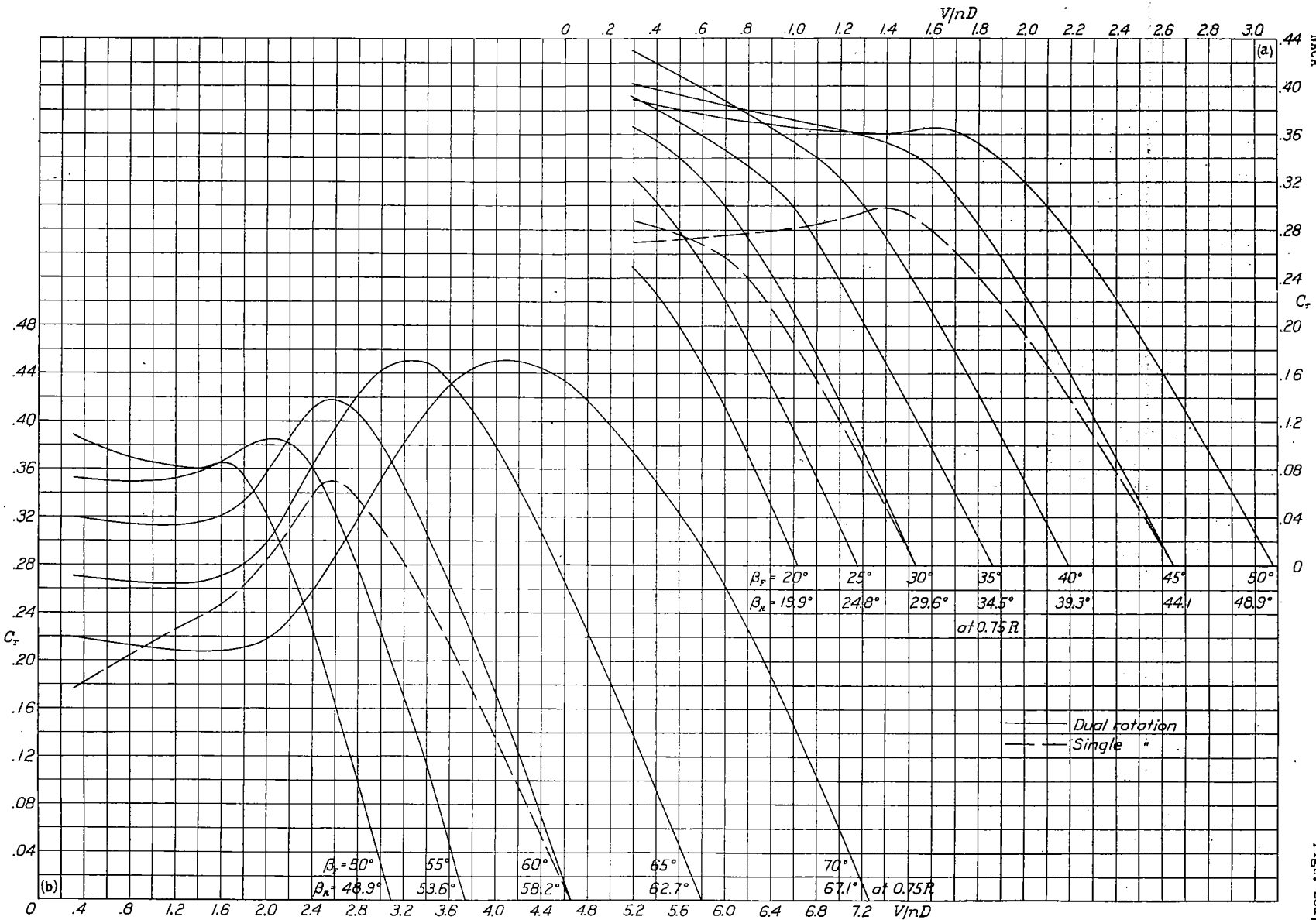


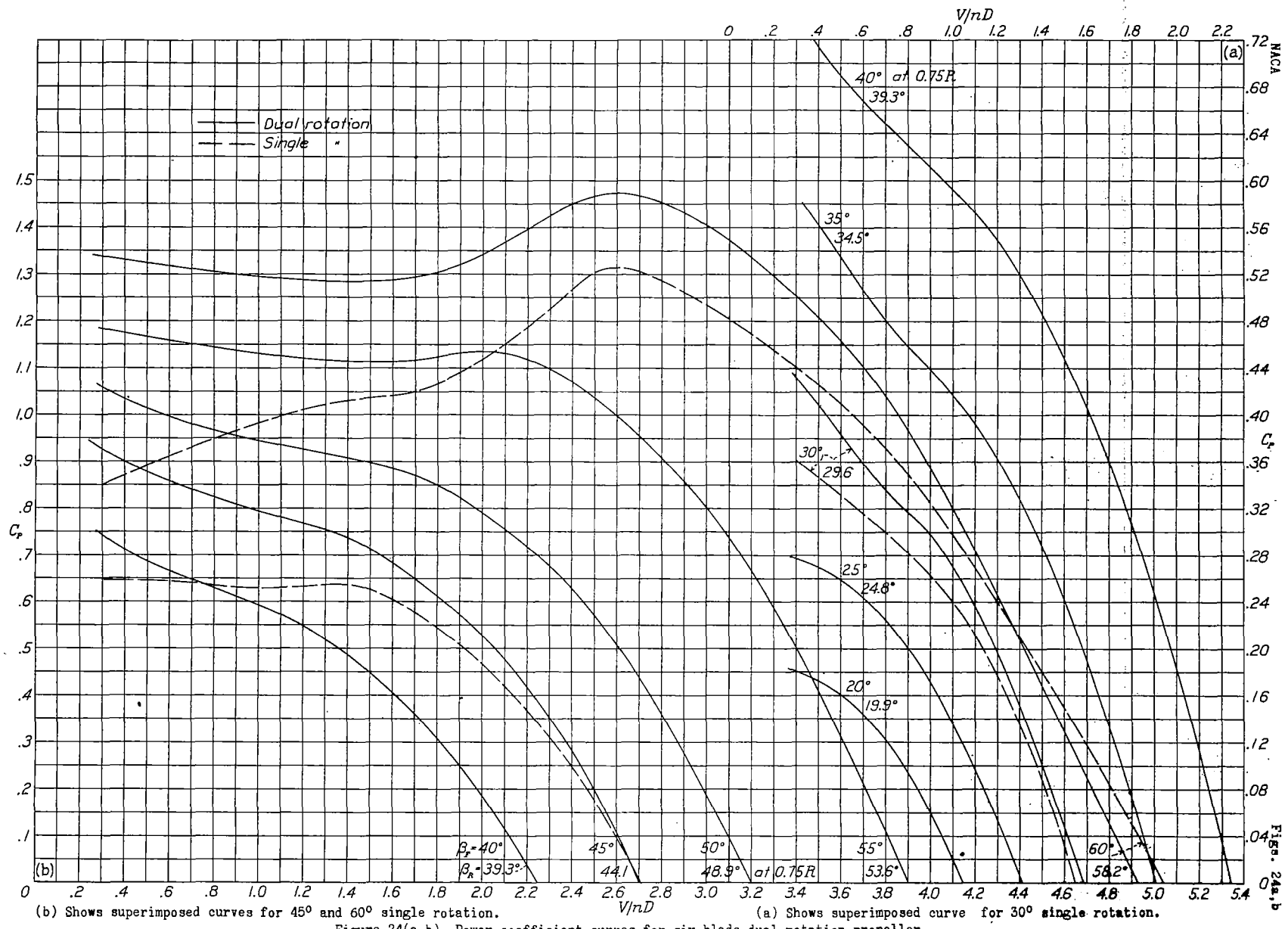
Figure 22.-Design chart for propeller 3155-6, six-blade single-rotation.



(b) Shows superimposed curve for 60° single rotation.

Figure 23(a,b).-Thrust-coefficient curves for six-blade dual-rotation propeller.

(a) Shows superimposed curves for 30° and 45° single rotation.



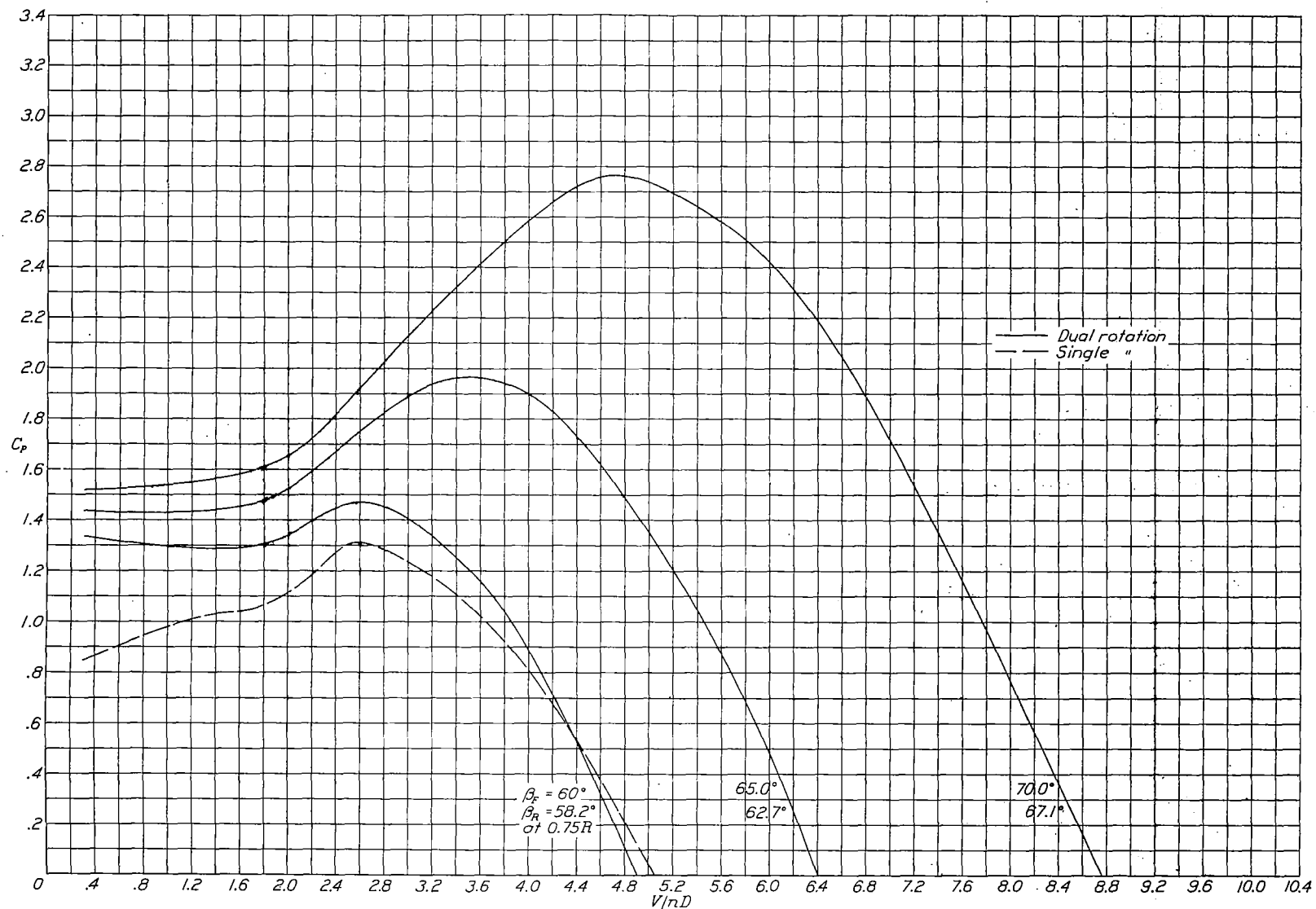


Figure 24(c).-Power-coefficient curves for six-blade dual-rotation propeller showing superimposed curve for 60° single rotation.

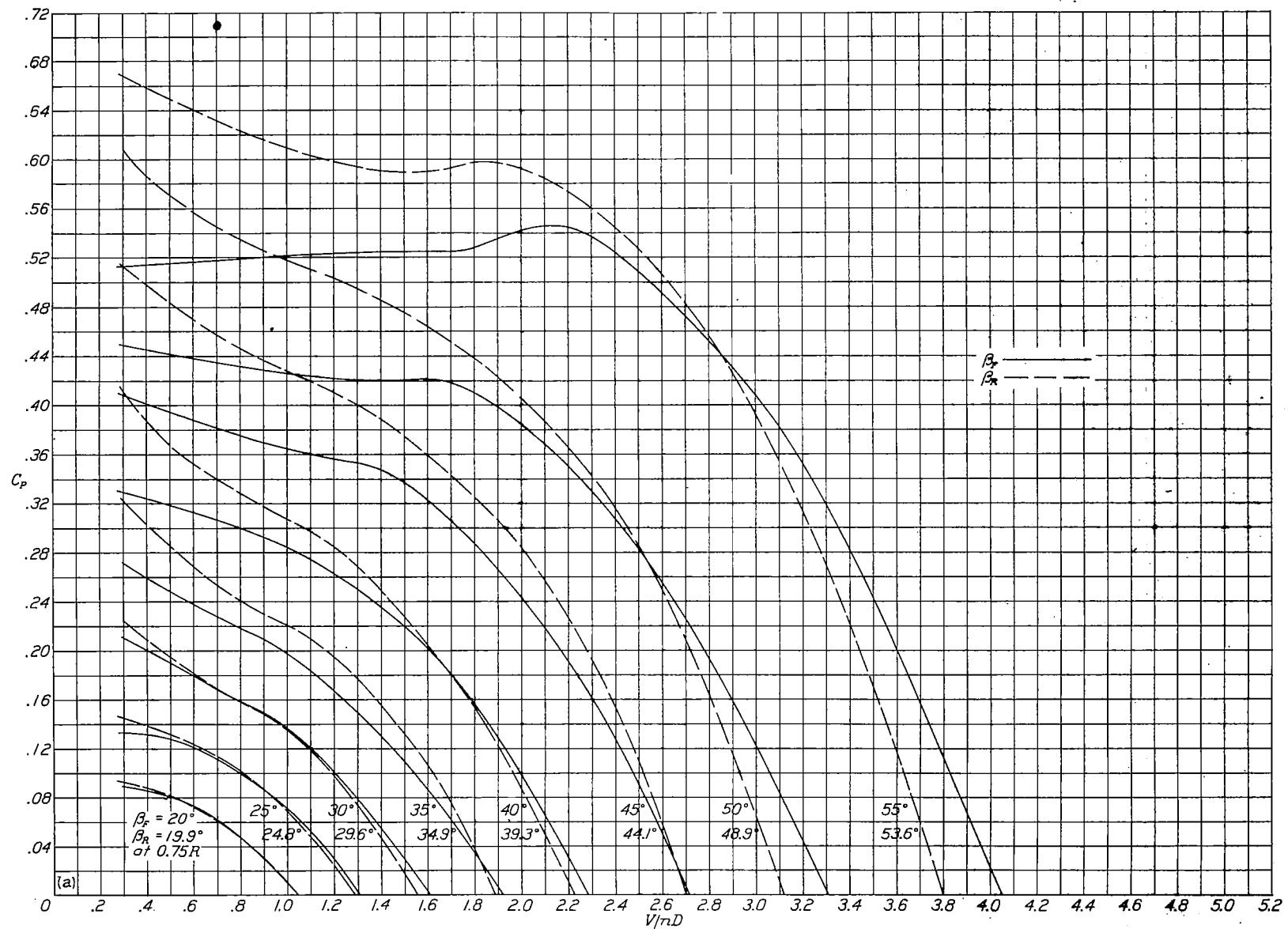


Figure 25(a).-Individual power-coefficient curves for six-blade dual-rotation propeller.

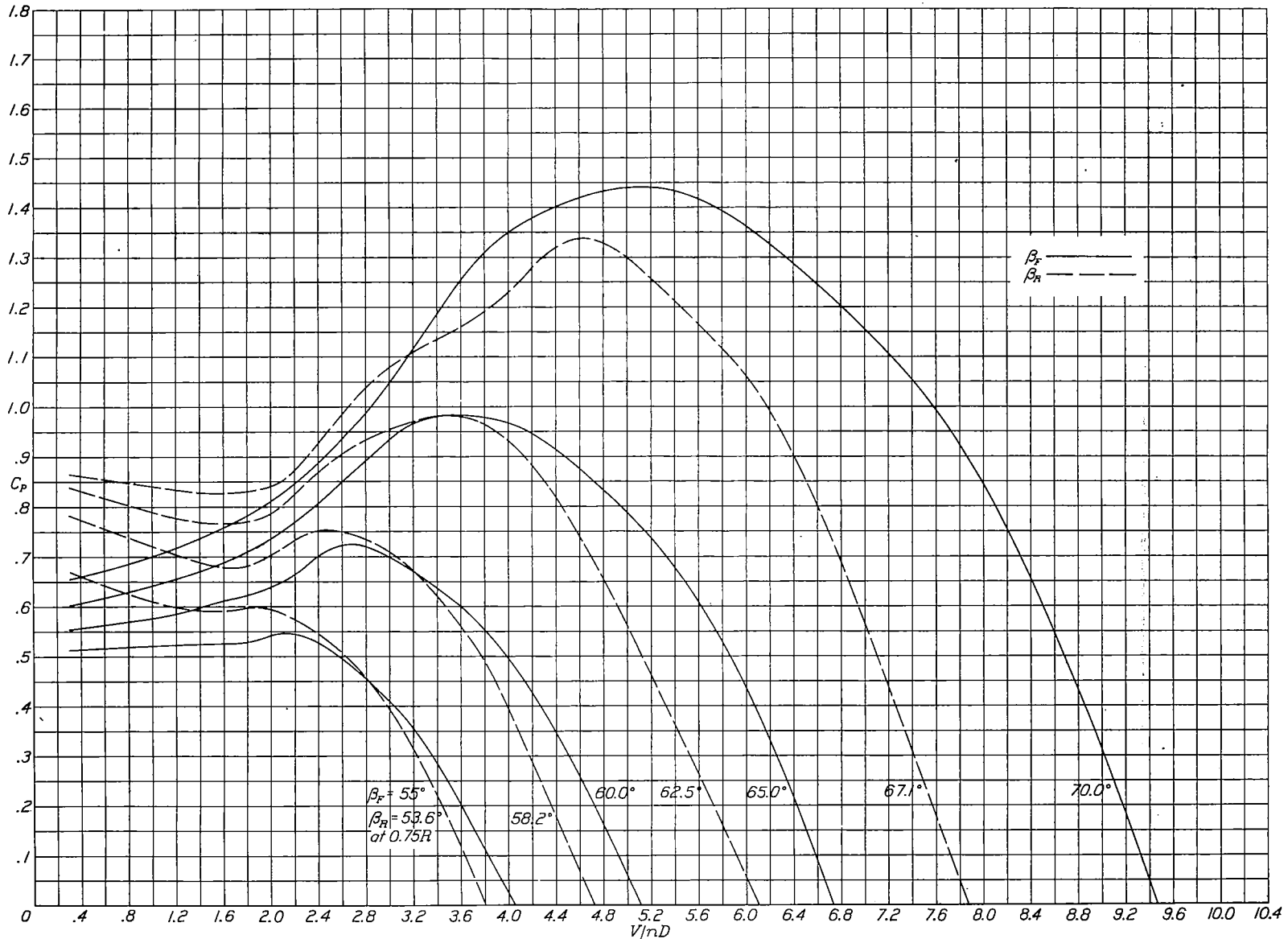


Figure 25(b).--Individual power-coefficient curves for six-blade dual-rotation propeller.

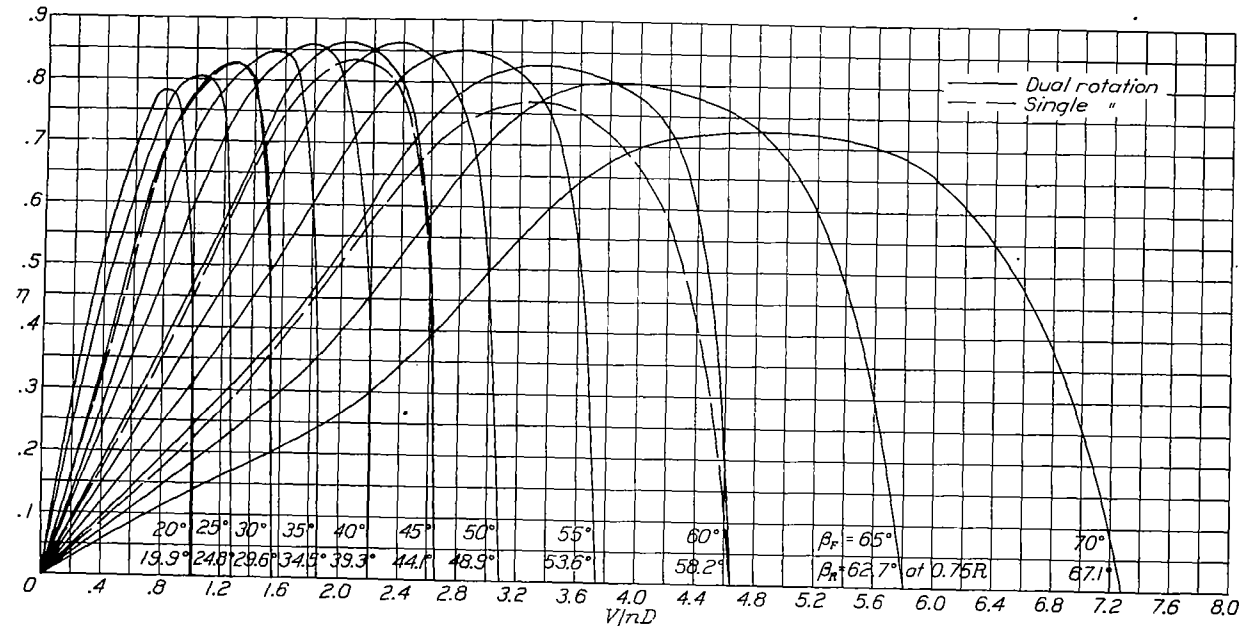


Figure 26.-Efficiency curves for six-blade dual-rotation propeller, showing superimposed curves for 30°, 45°, and 60° single rotation.

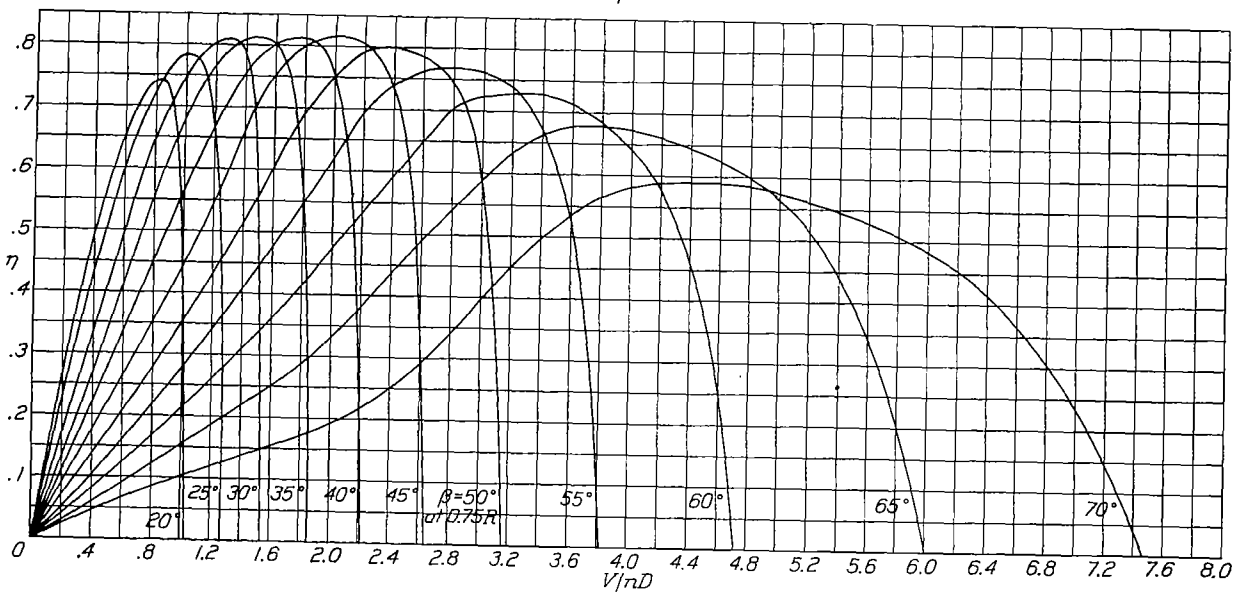


Figure 30.- Efficiency curves for eight-blade single-rotation propeller.

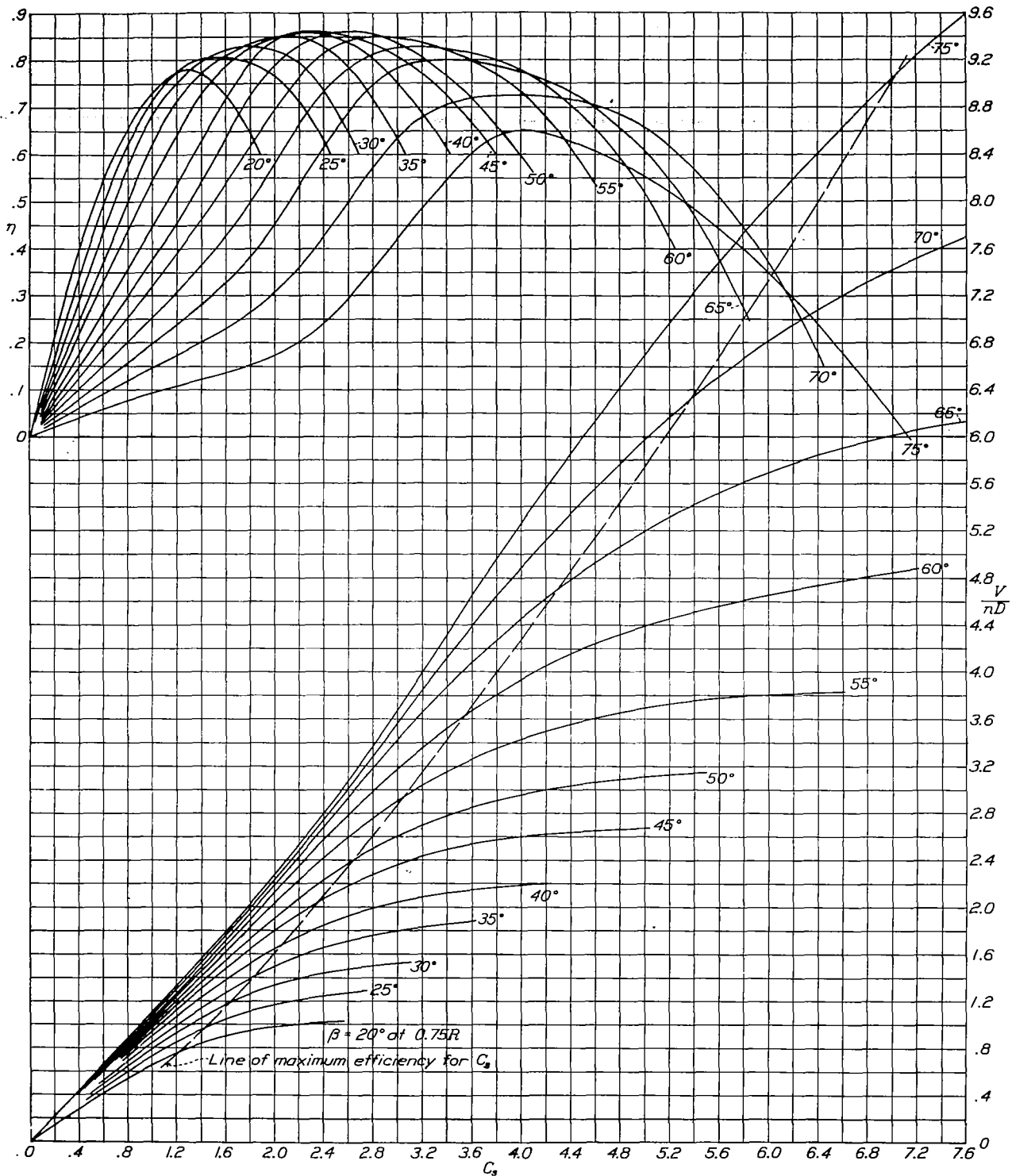


Figure 27.-Design chart for propellers 3155-6(R.H.) and 3156-6(L.H.), six-blade dual rotation.

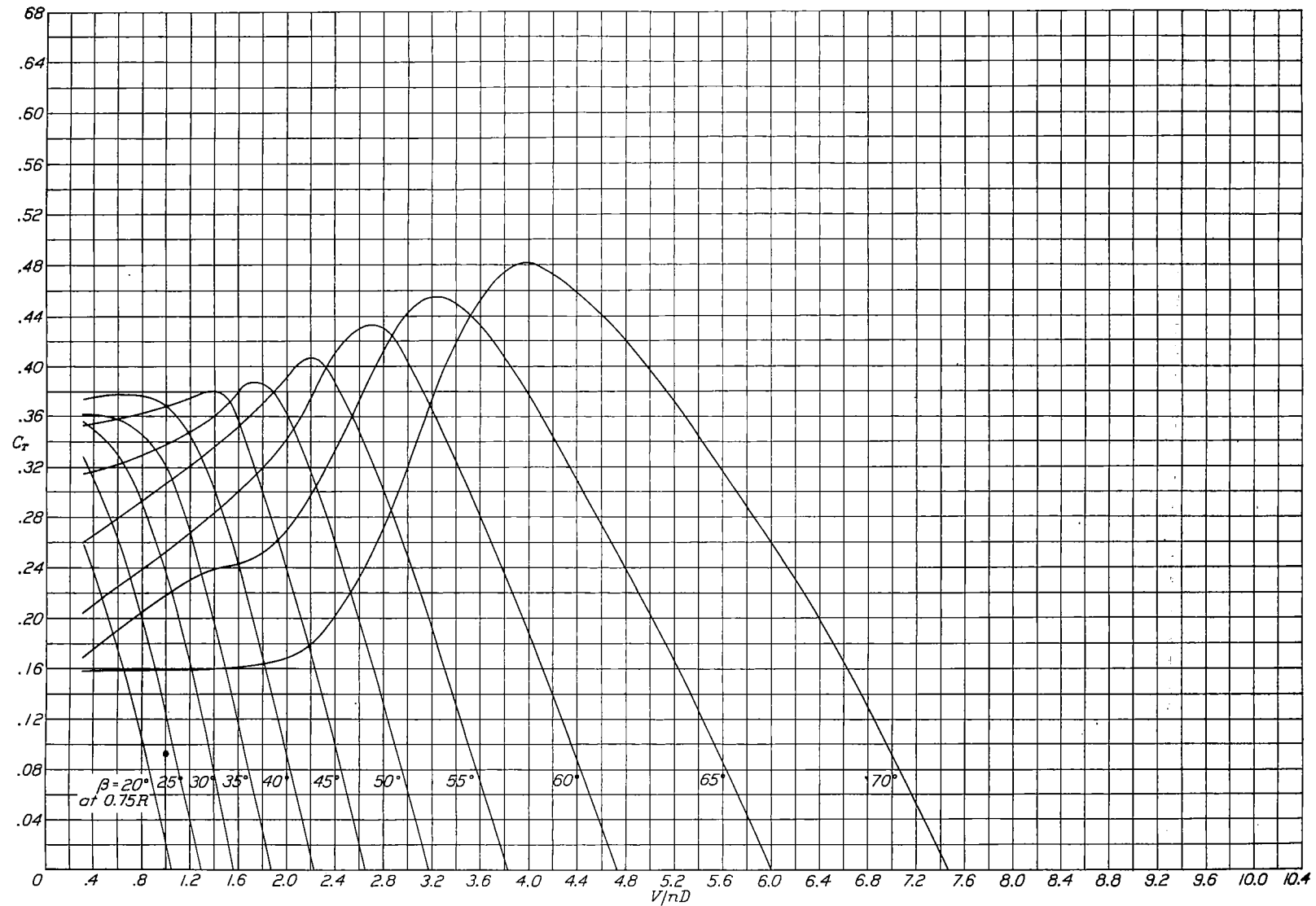


Figure 28.-Thrust-coefficient curves for eight-blade single-rotation propeller.

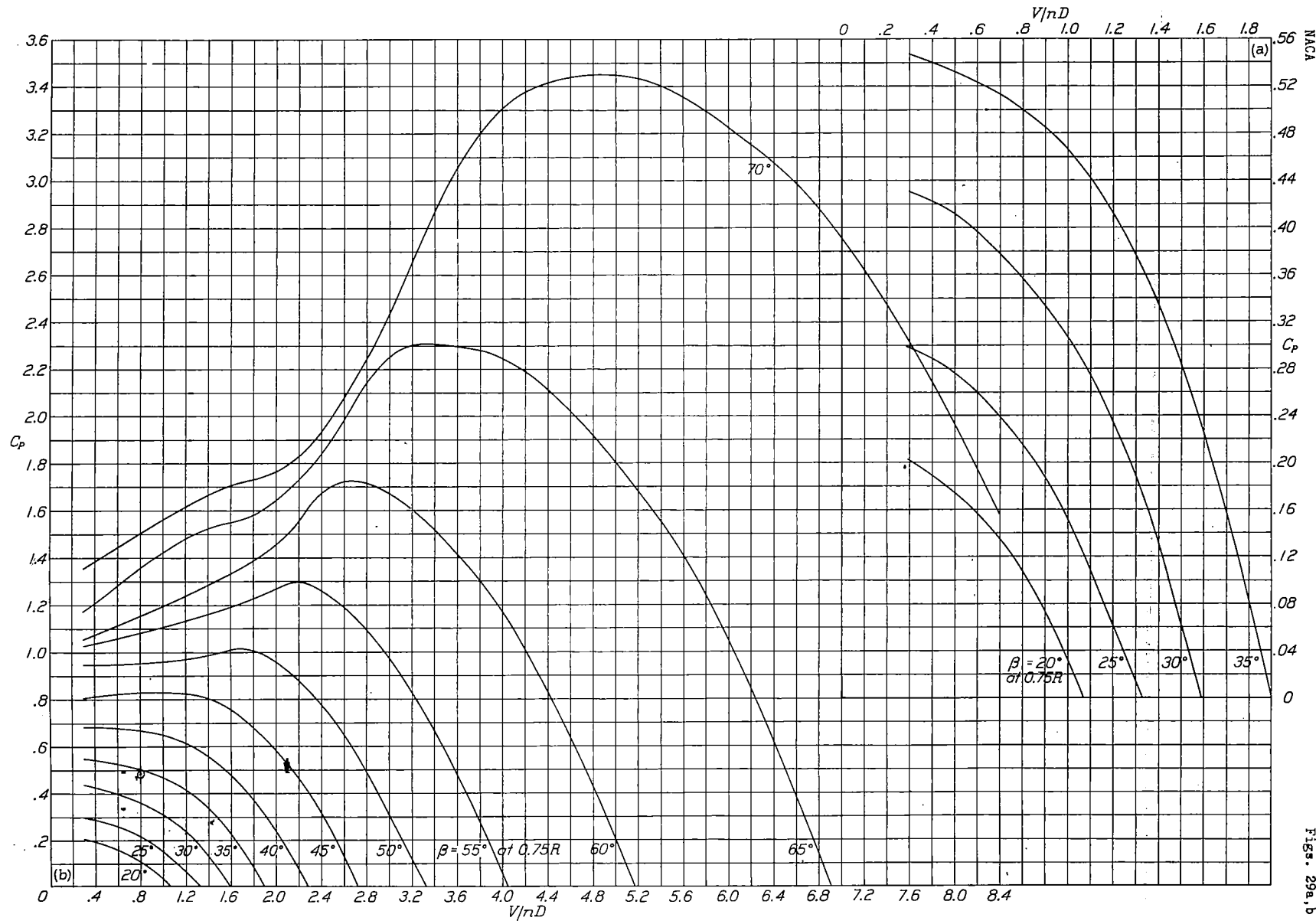


Figure 29(a,b).-Power-coefficient curves for eight-blade single-rotation propeller.

FIGS. 29a, b

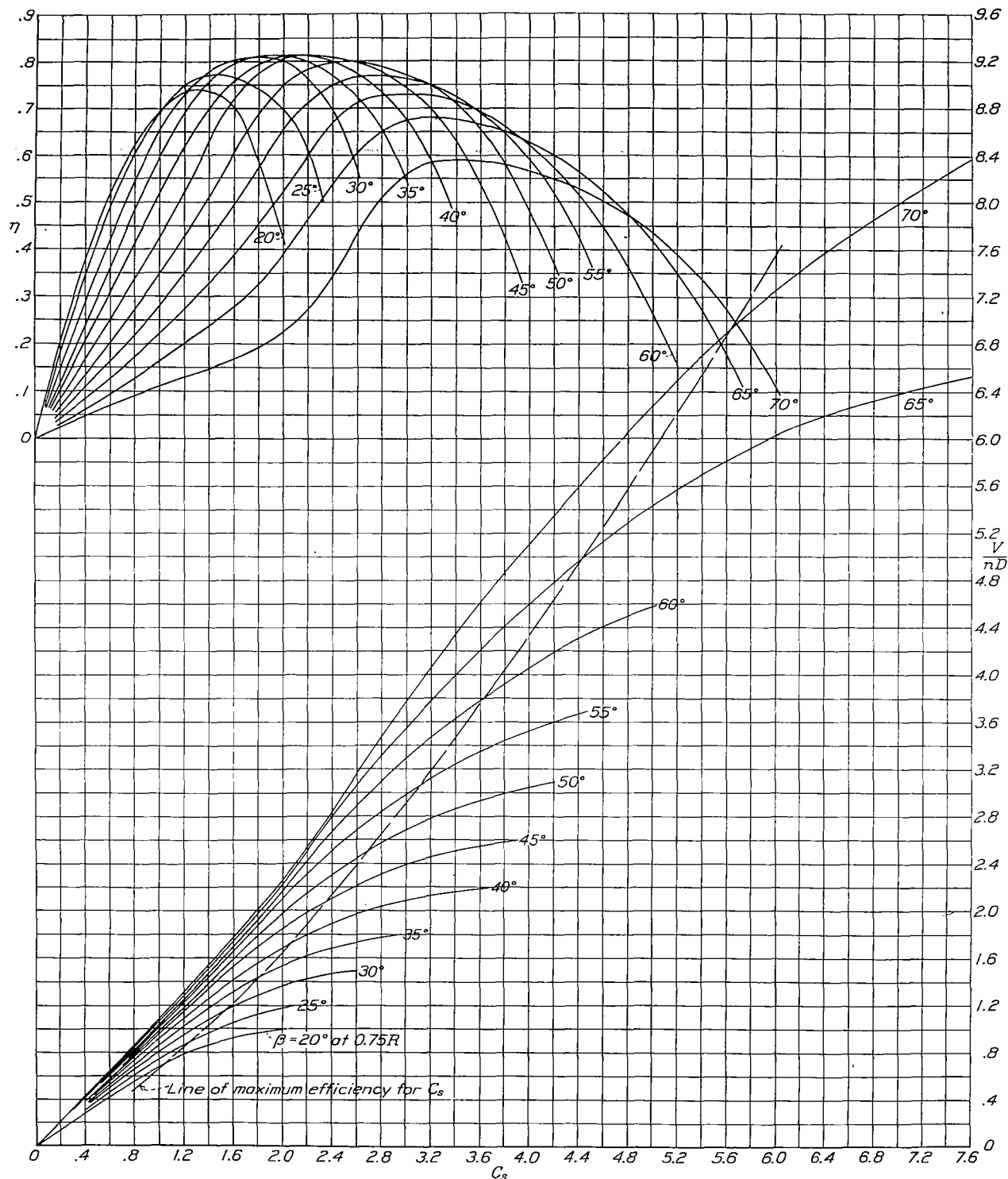


Figure 31.-Design chart for propeller 3155-6(R.H.), eight blade, single rotation.

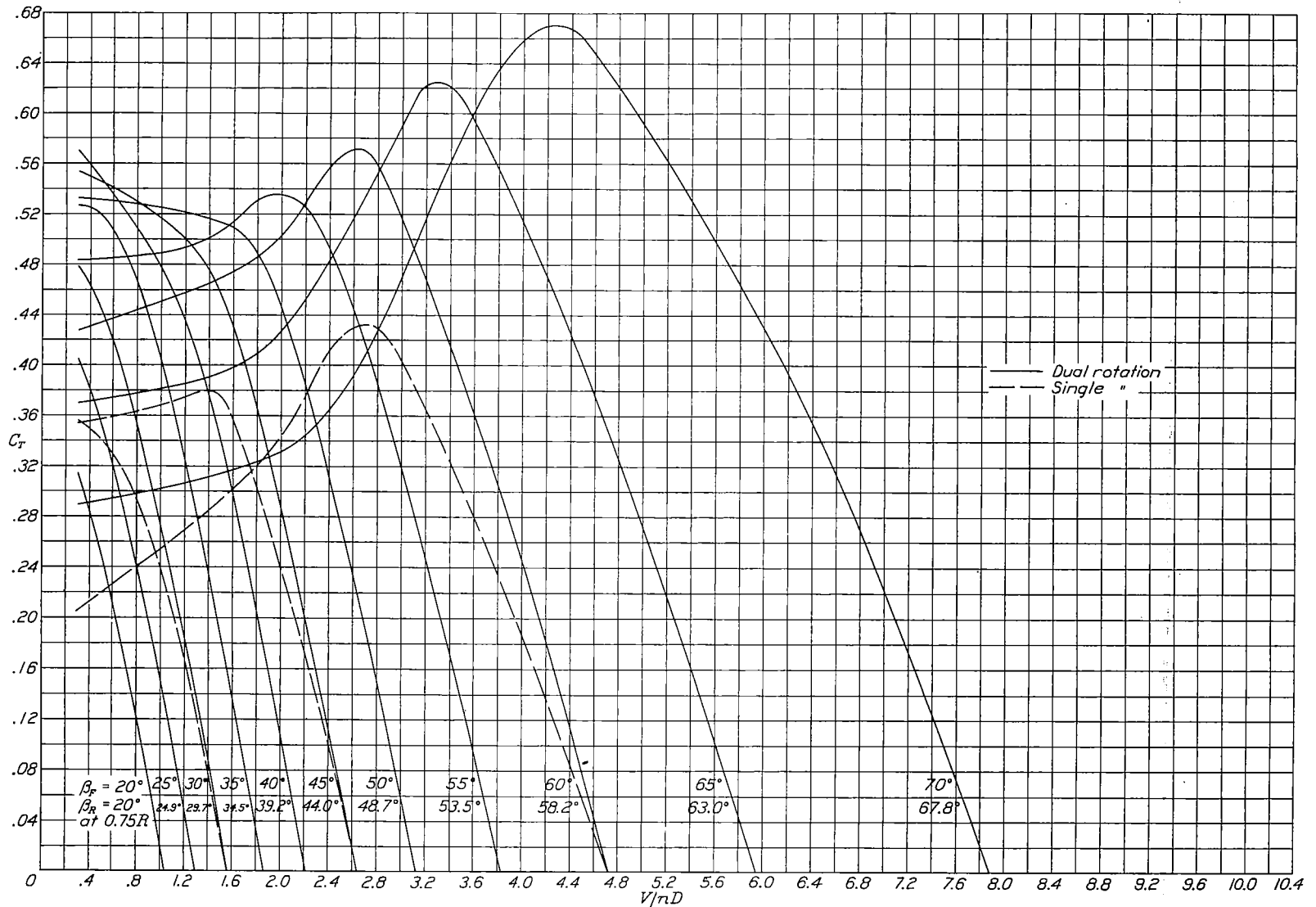
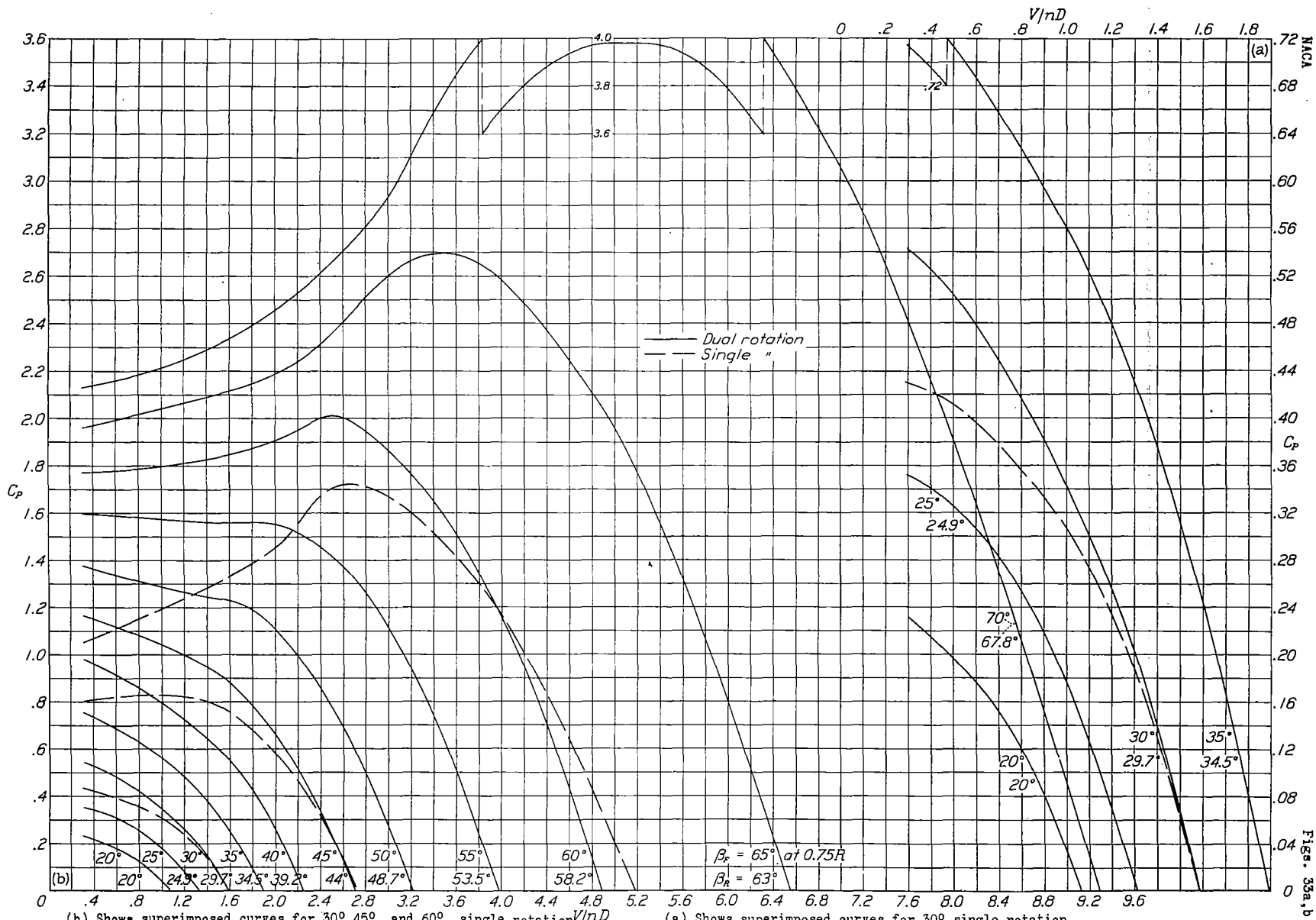


Figure 32.-Thrust-coefficient curves for eight-blade dual-rotation propeller, showing superimposed curves for 30° , 45° , and 60° , single rotation.



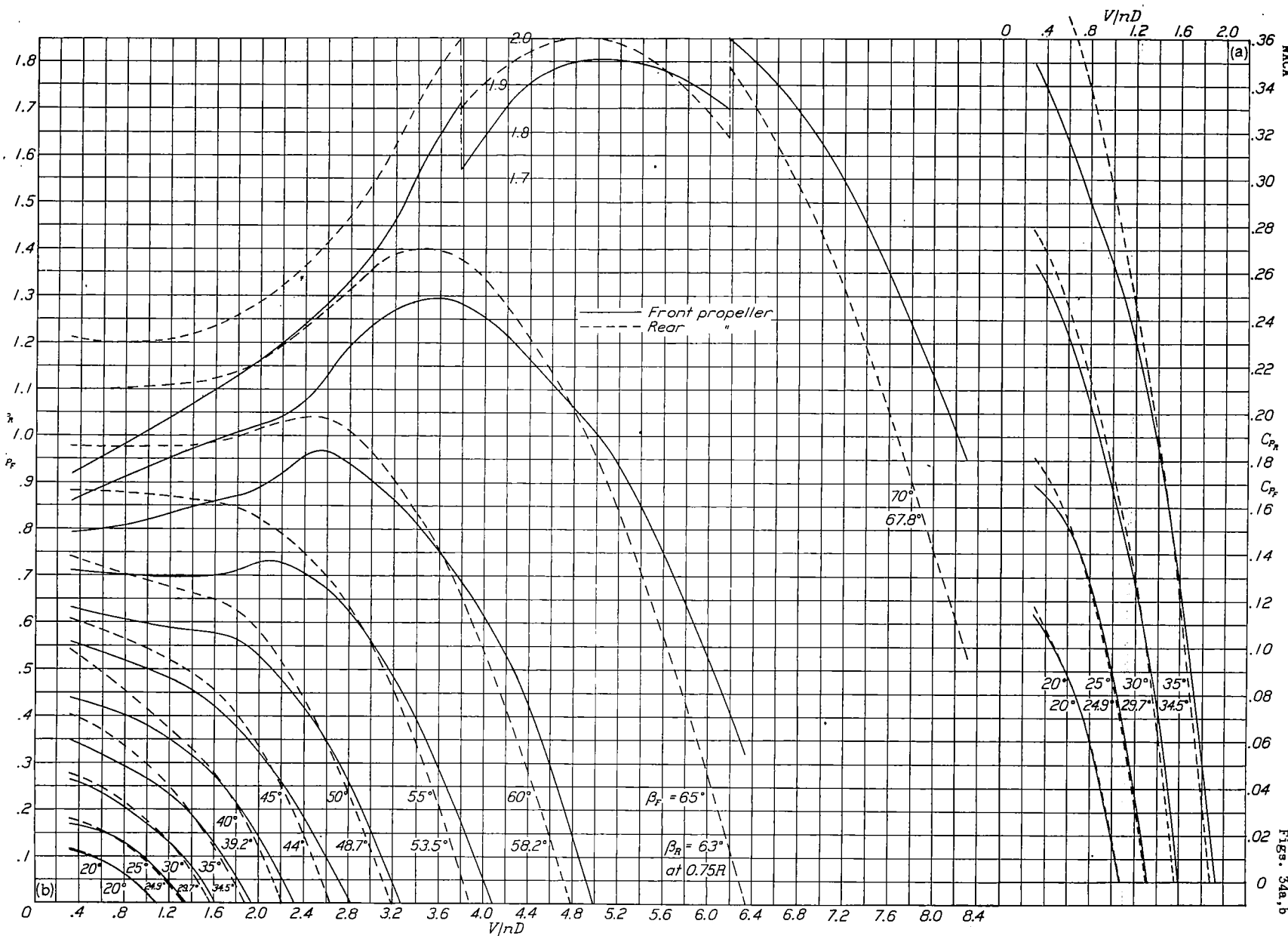


Figure 34(a,b).-Individual power-coefficient curves for eight-blade dual-rotation propeller.

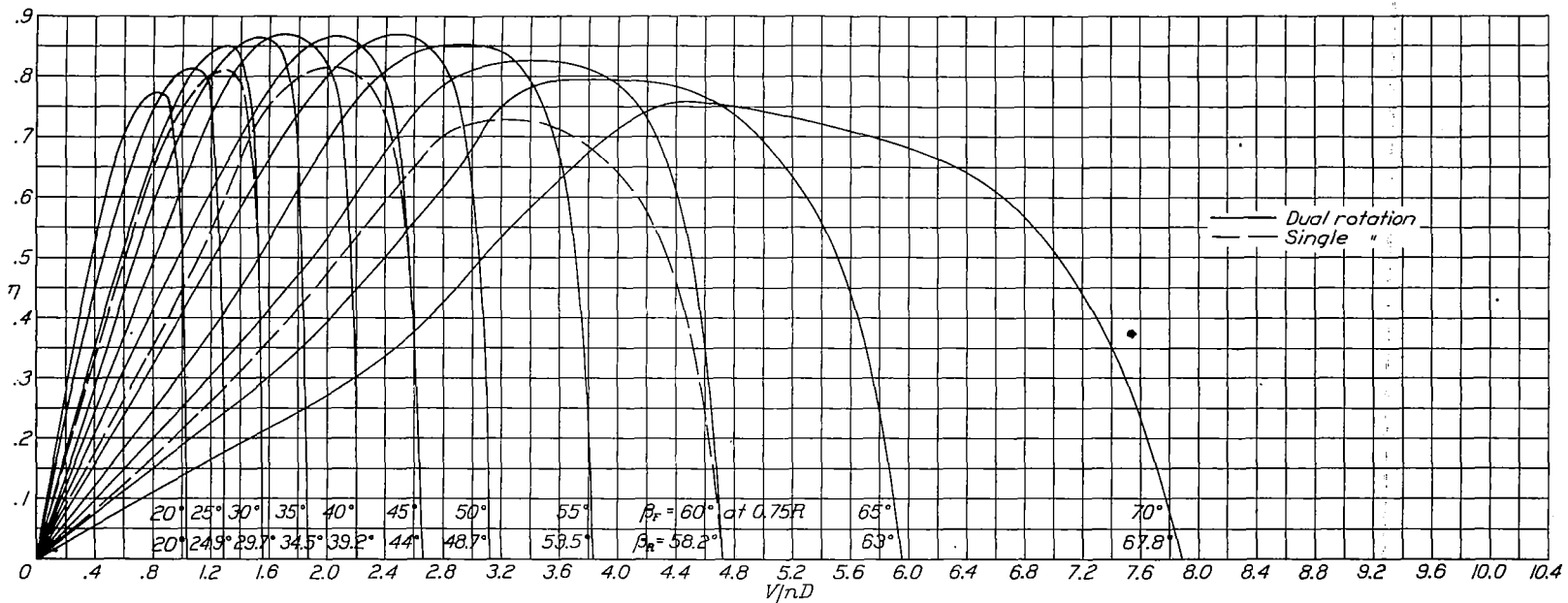


Figure 35.-Efficiency curves for eight-blade dual-rotation propeller, showing superimposed curves for 30°, 45°, and 60°, single rotation.

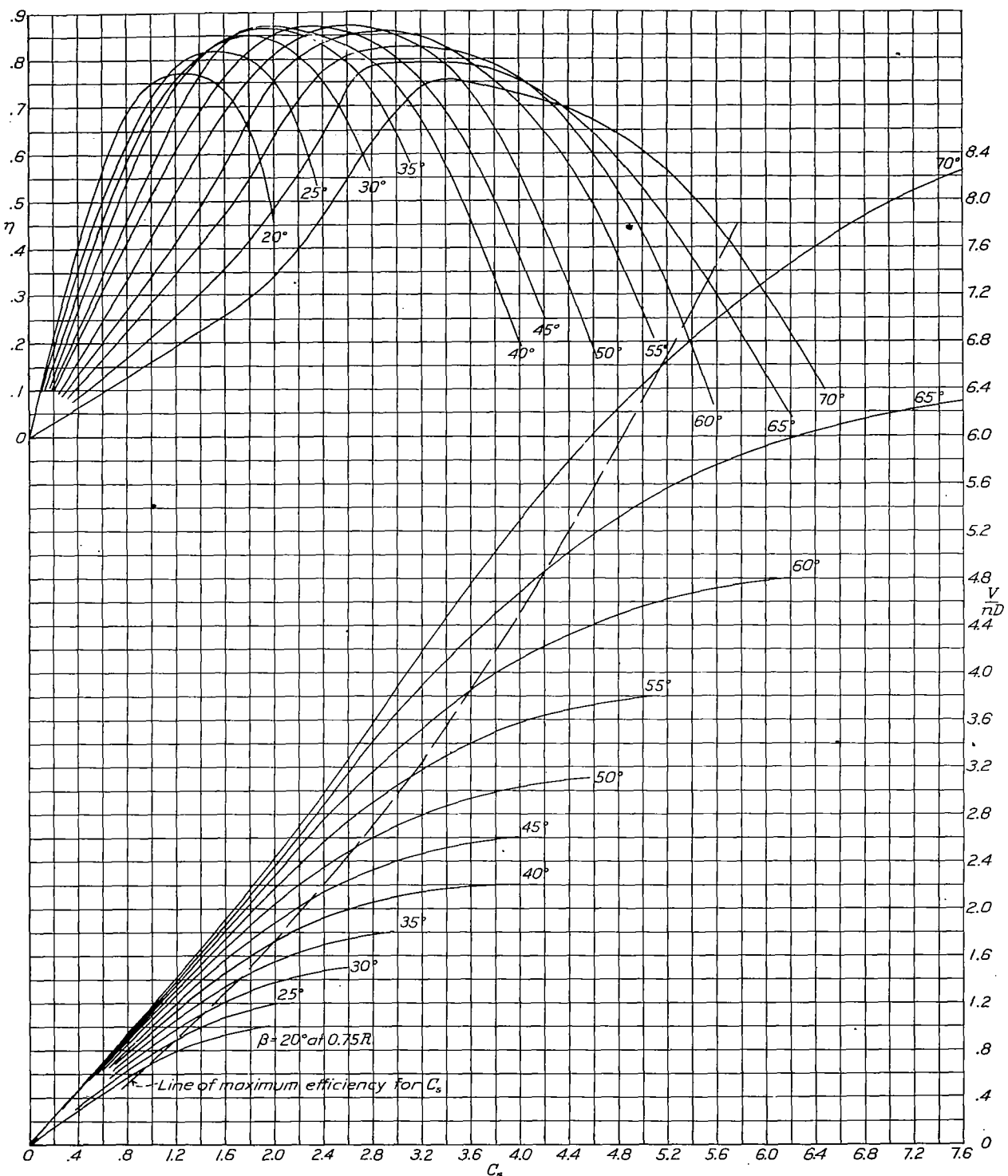


Figure 36.-Design chart for propellers 3155-6(R.H.) and 3156-6(L.H.) eight blade dual rotation.

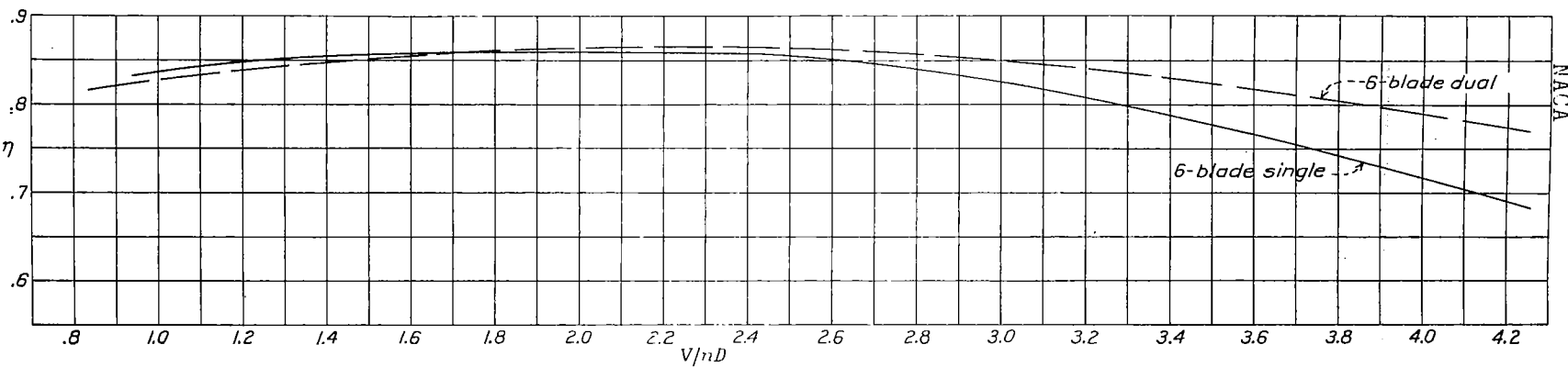


Figure 37.-Net efficiency envelope comparison for long spinner rotating.

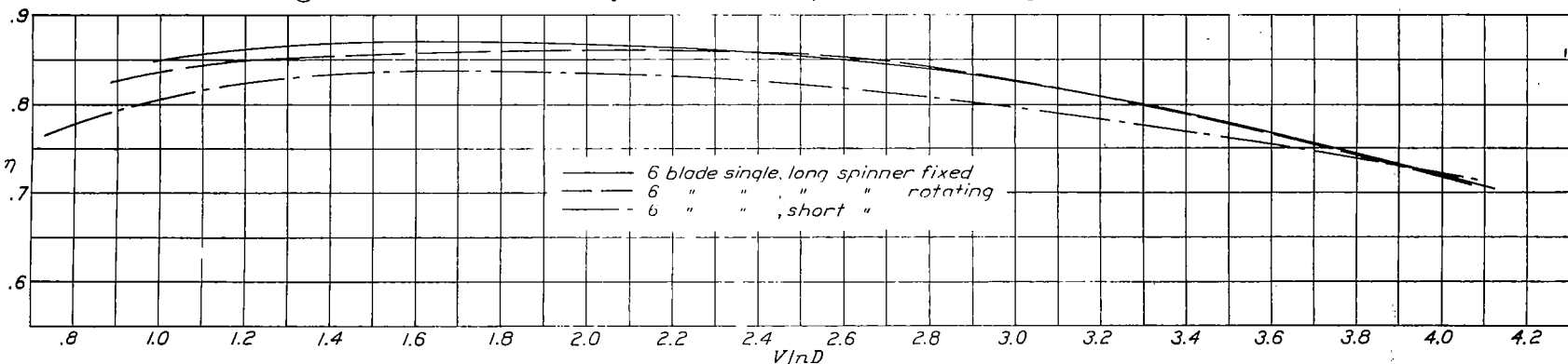


Figure 38.-Net efficiency envelope comparisons for long and short spinner, six-blade single rotation.

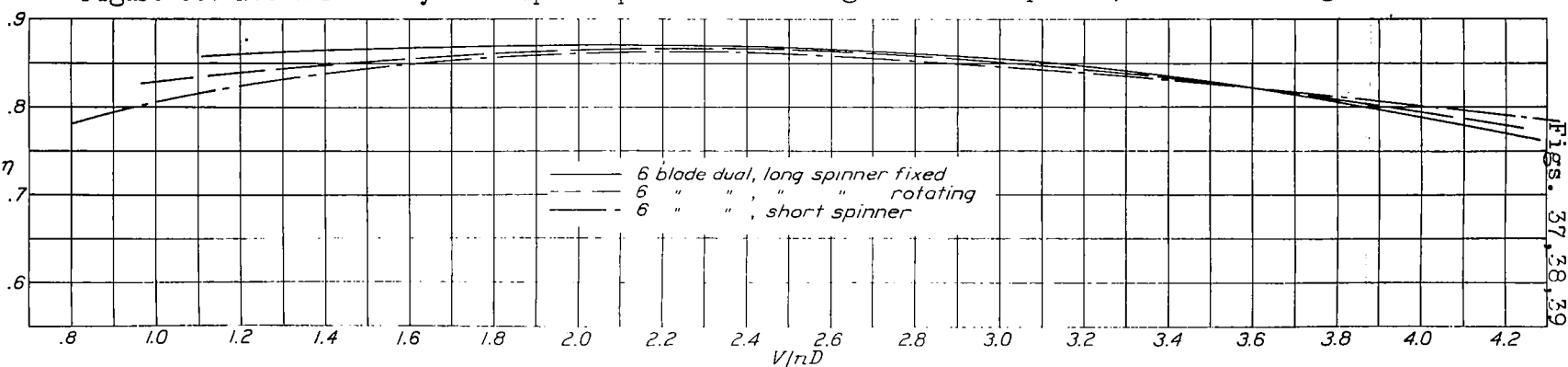


Figure 39.-Net efficiency envelope comparison for long and short spinner, six-blade dual rotation.

NACA

Figs. 37
38
39

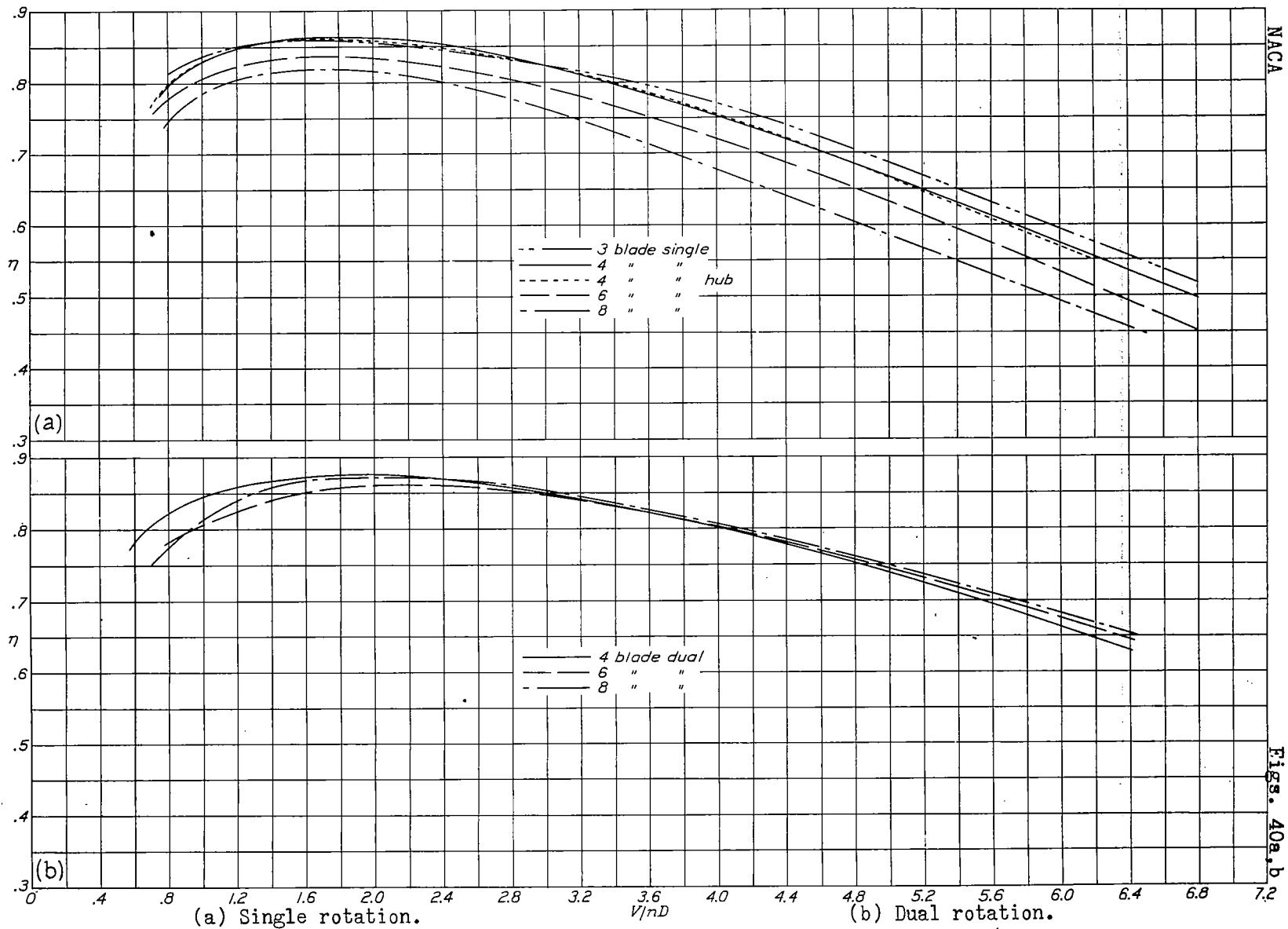


Figure 40(a,b).-Efficiency envelope comparisons for different solidities.

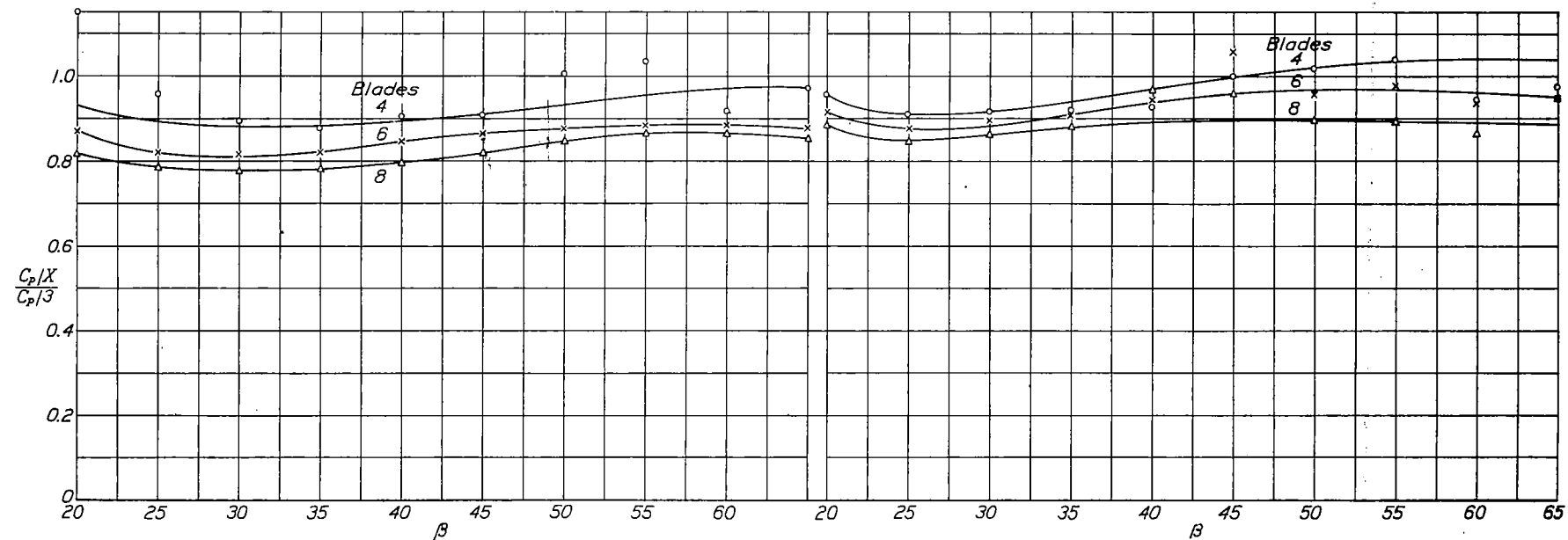


Fig. 41.- Single rotation.

Fig. 42.- Dual rotation.

Figures 41, 42.- Ratio of power absorbed per blade at peak efficiency to that of a three-blade propeller.

1
65
8

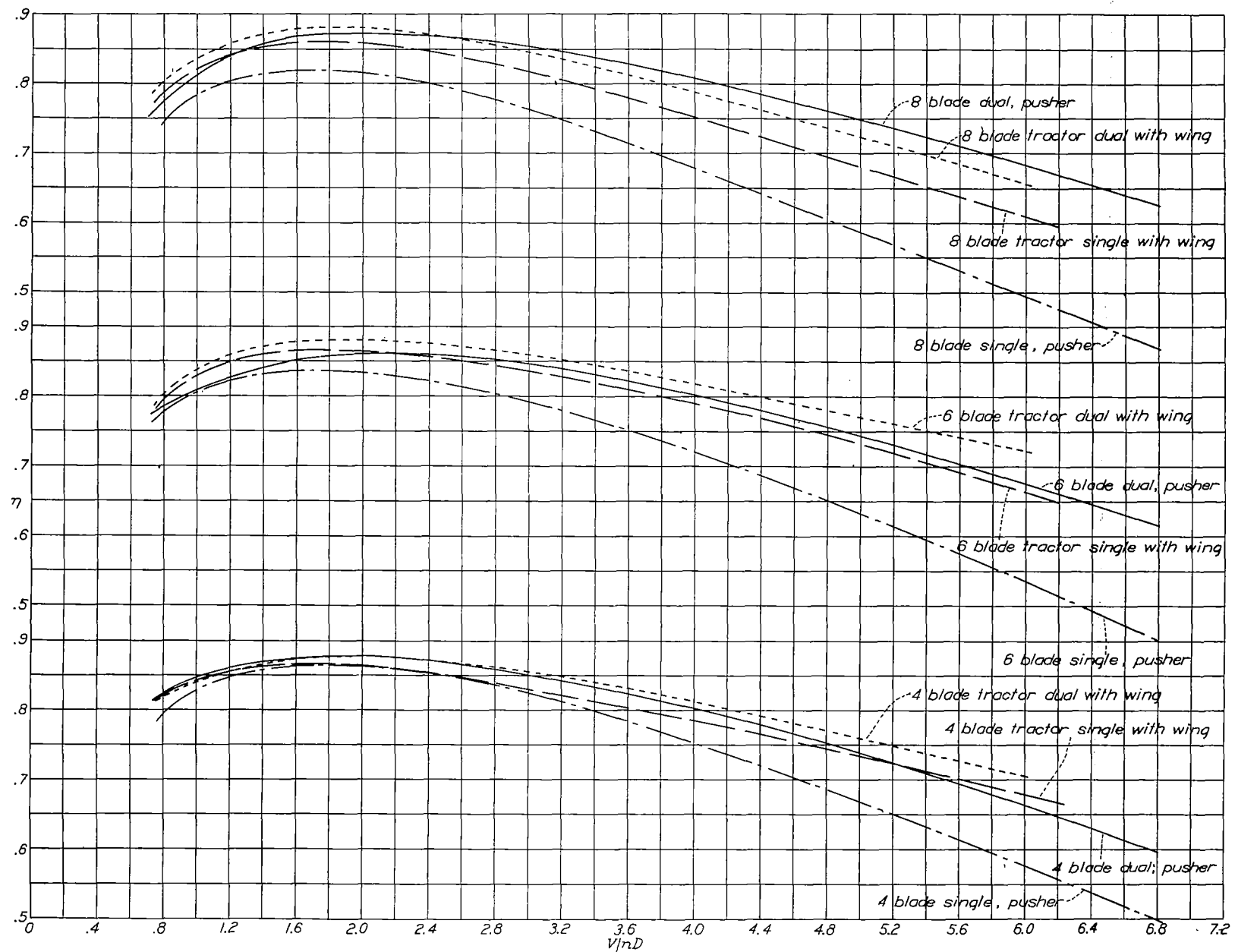


Figure 43.-Effect of dual rotation on efficiency envelopes for tractor and pusher propellers.

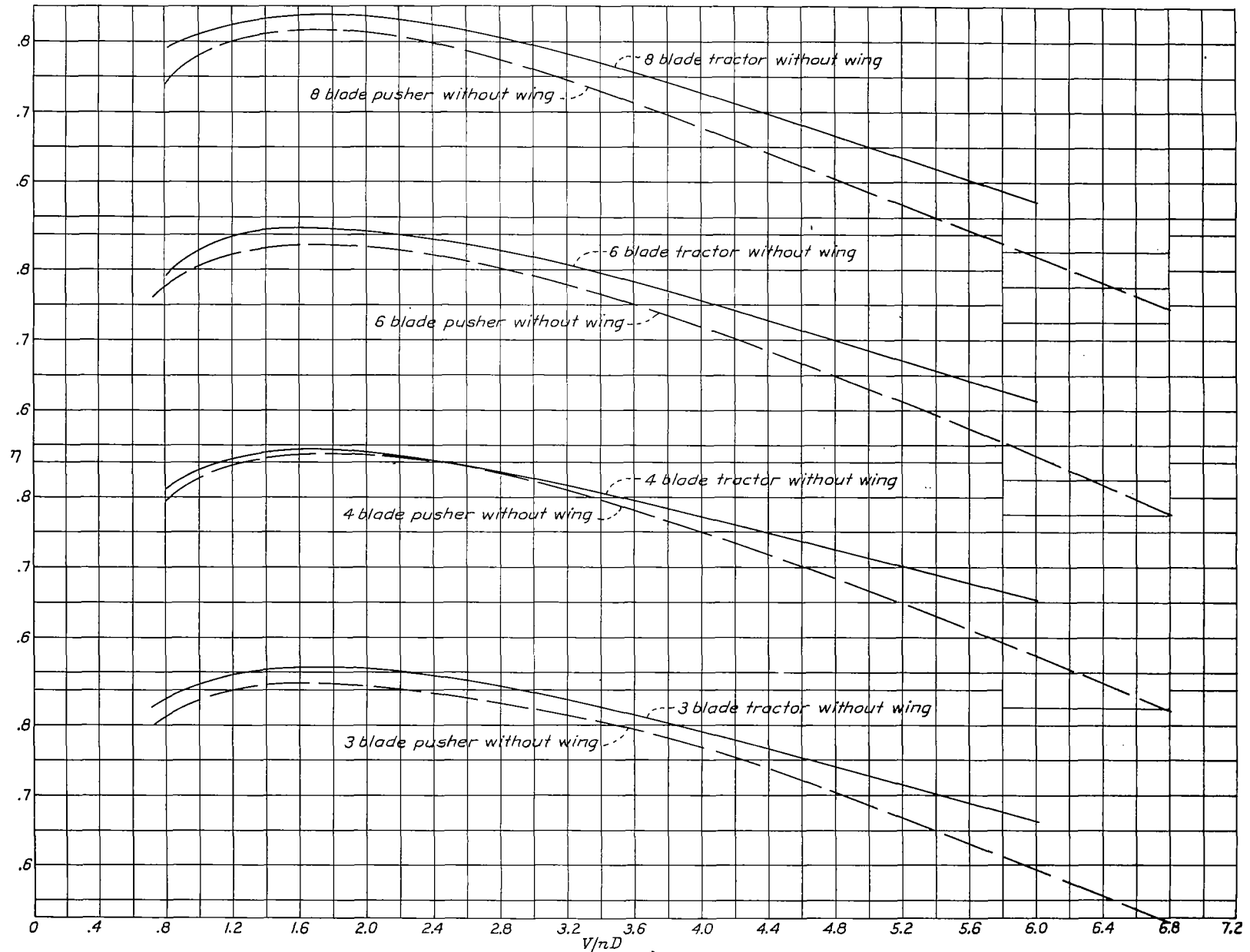


Figure 44.-Comparison of efficiency envelopes for tractor and pusher propellers, single rotation without wing.

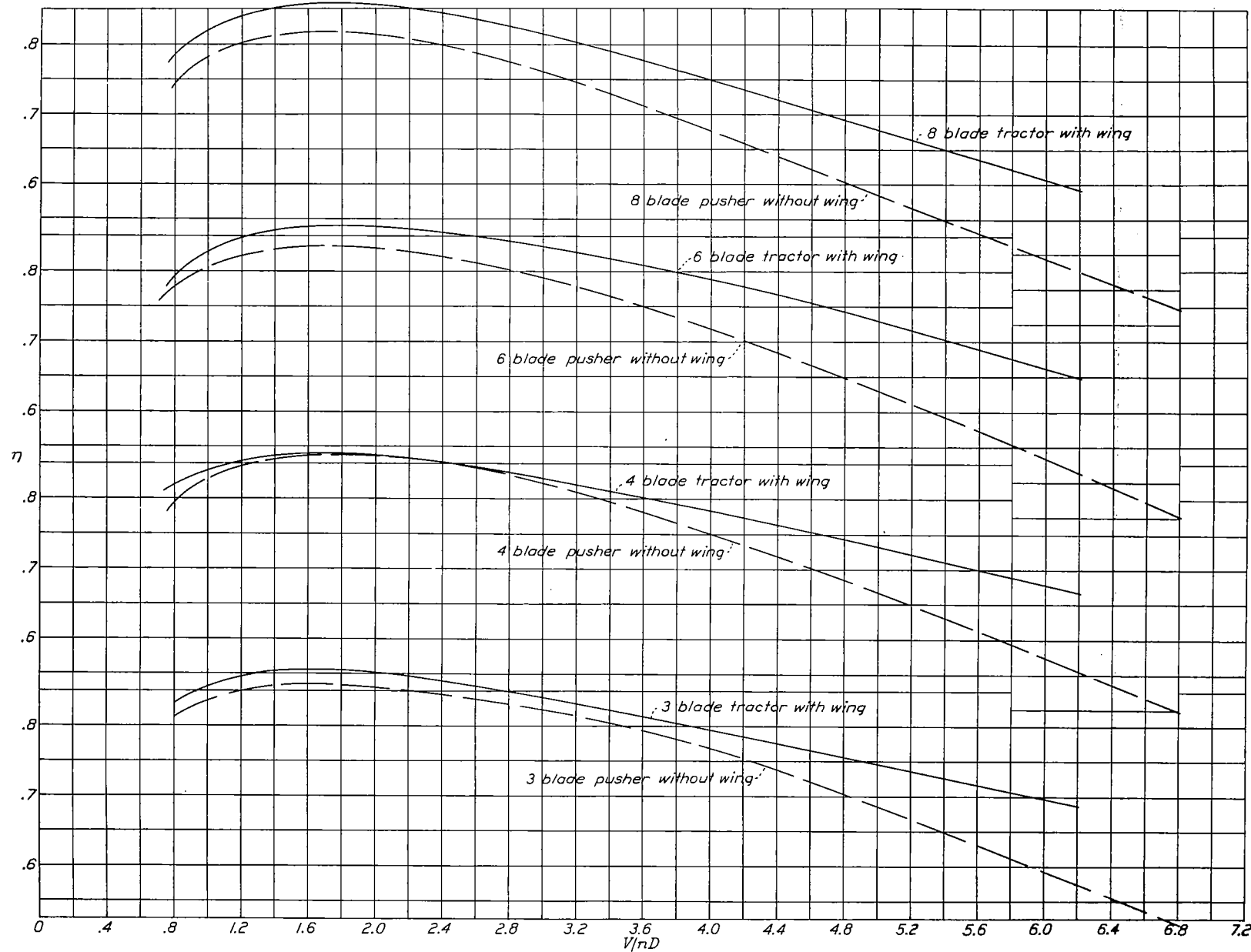


Figure 45.-Comparison of efficiency envelopes for tractor and pusher propellers, single rotation.

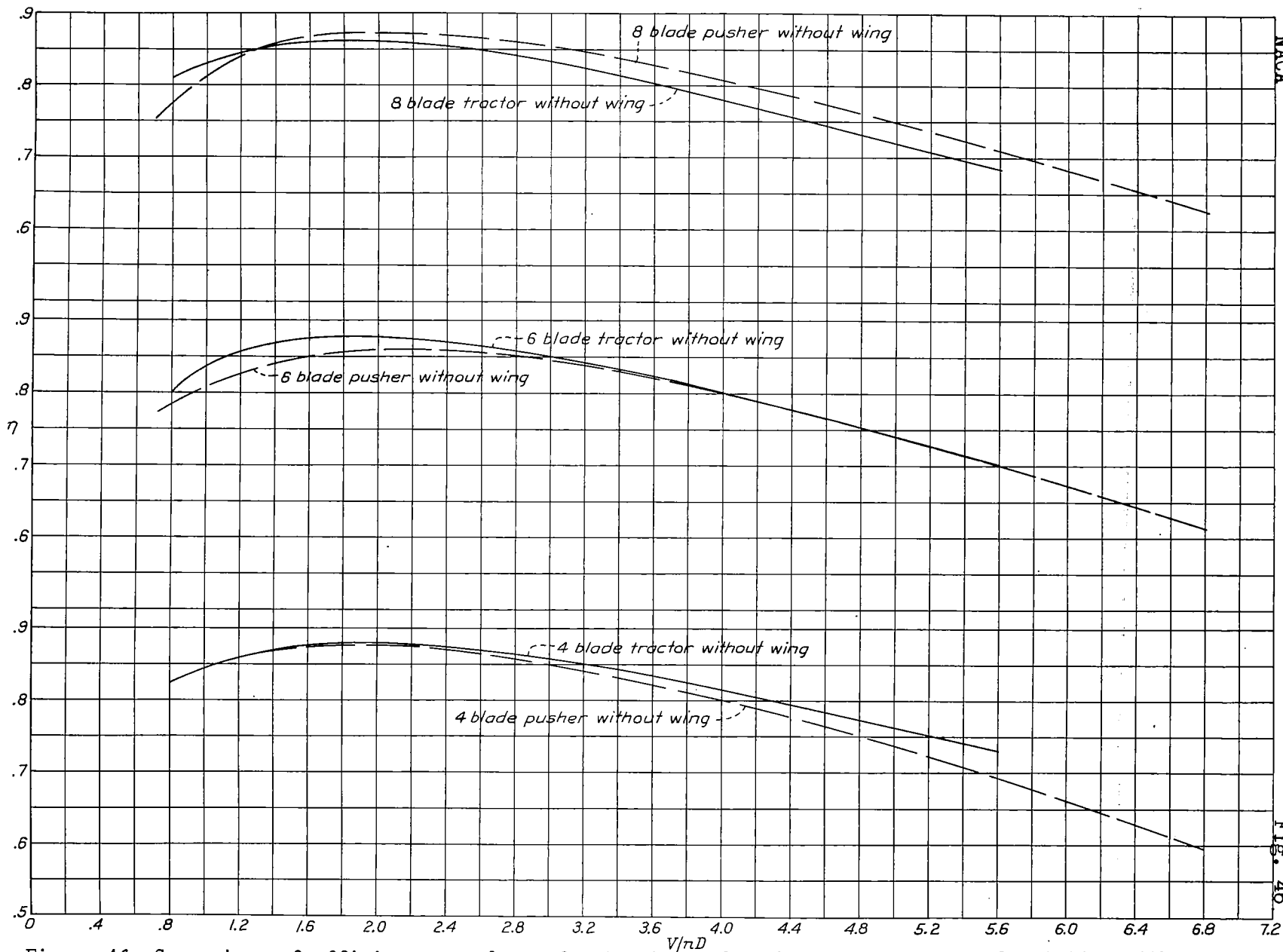


Figure 46.-Comparison of efficiency envelopes for tractor and pusher propellers, dual rotation without wing.

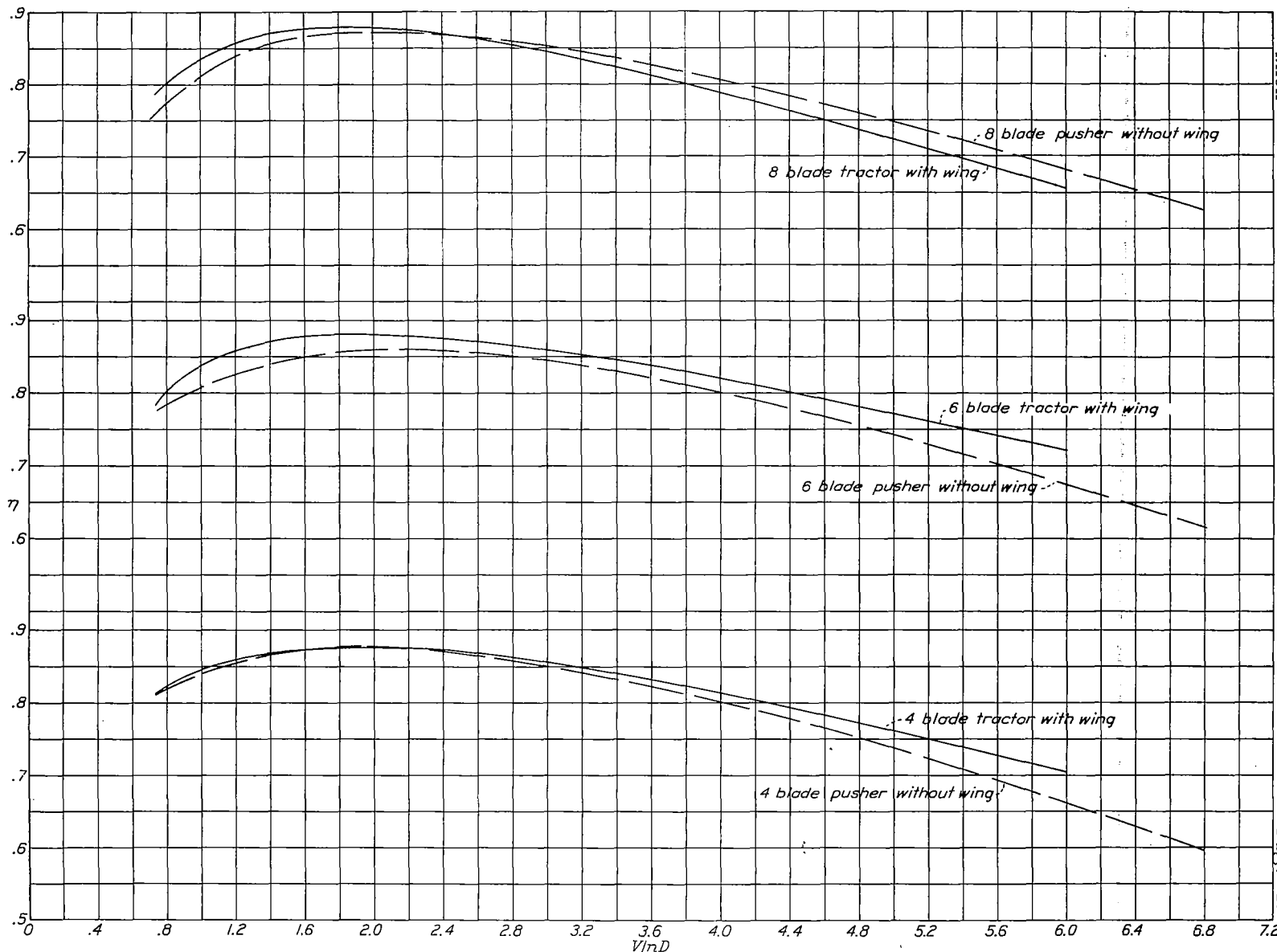
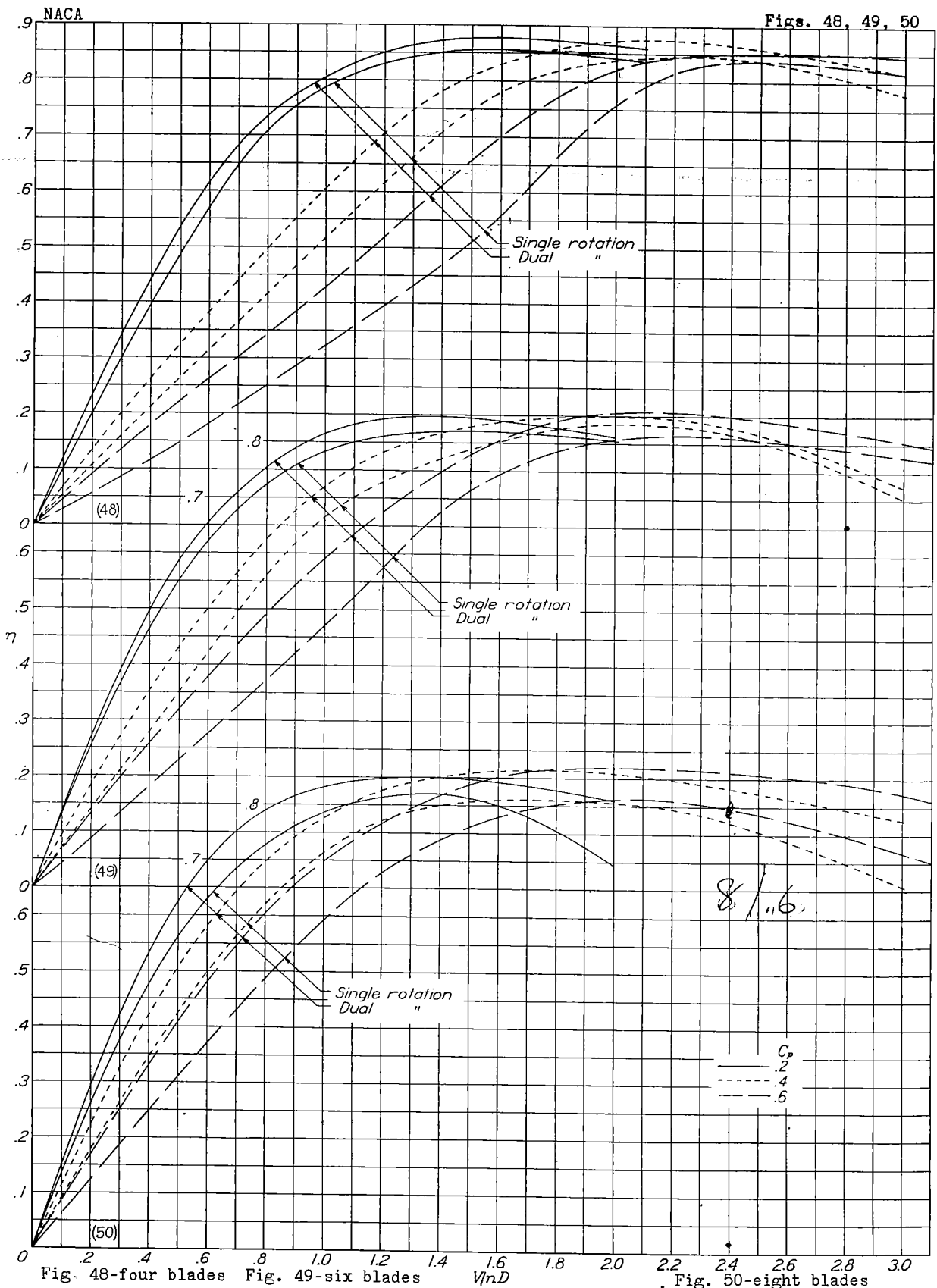


Figure 47.-Comparison of efficiency envelopes for tractor and pusher propellers, dual rotation.



Figures 48, 49, 50.- Effect of dual rotation on efficiency for propellers at constant power.

NACA

Figs. 54,55

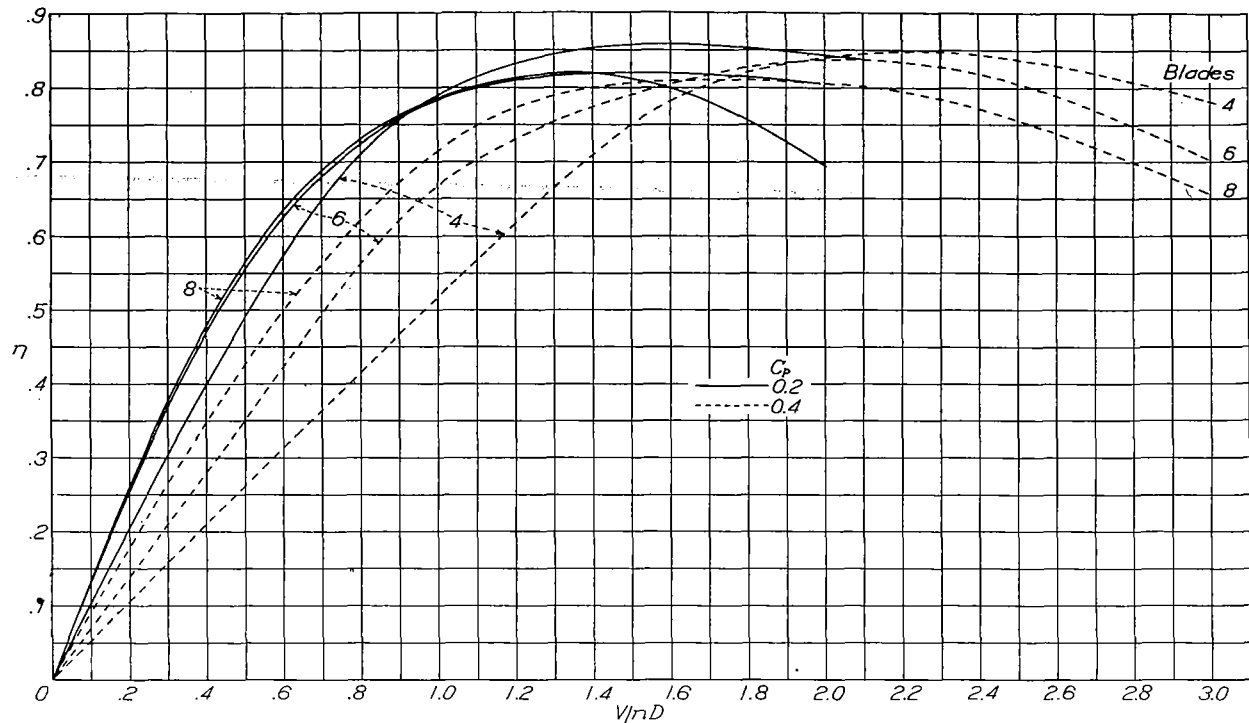


Figure 54.-Effect of solidity on efficiency for single rotation at constant power.

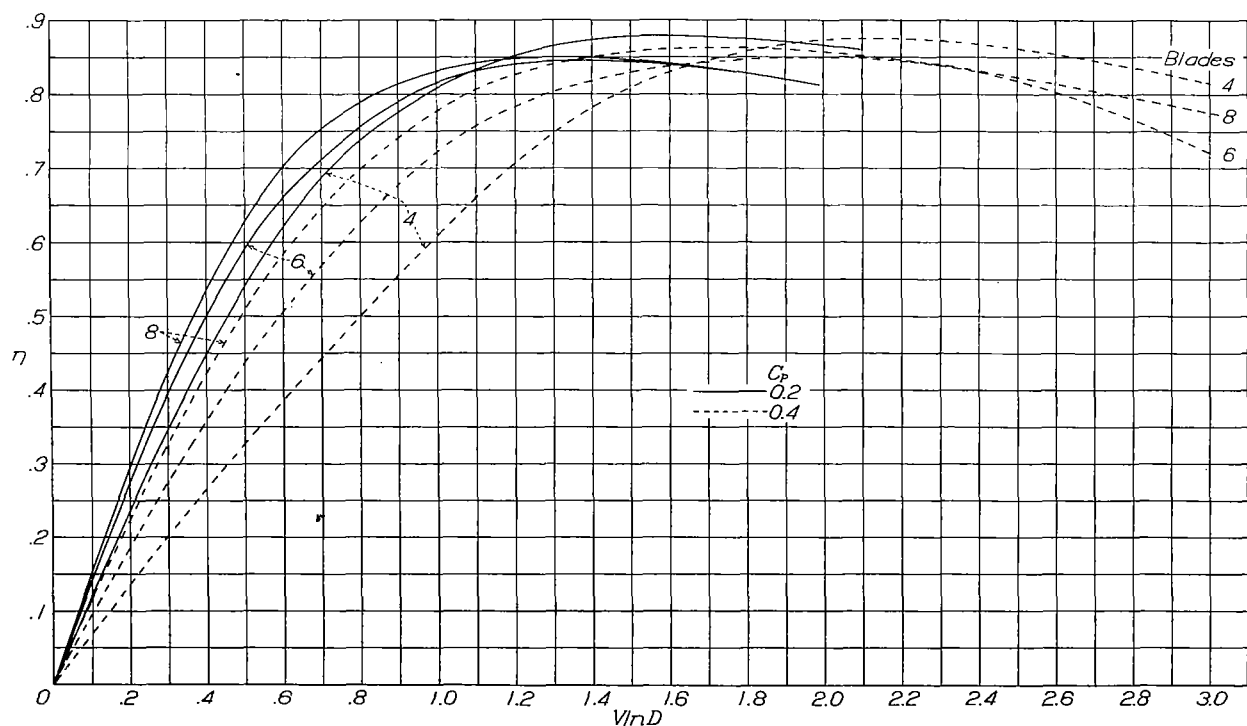


Figure 55.-Effect of solidity on efficiency for dual rotation at constant power.

Fig. 57

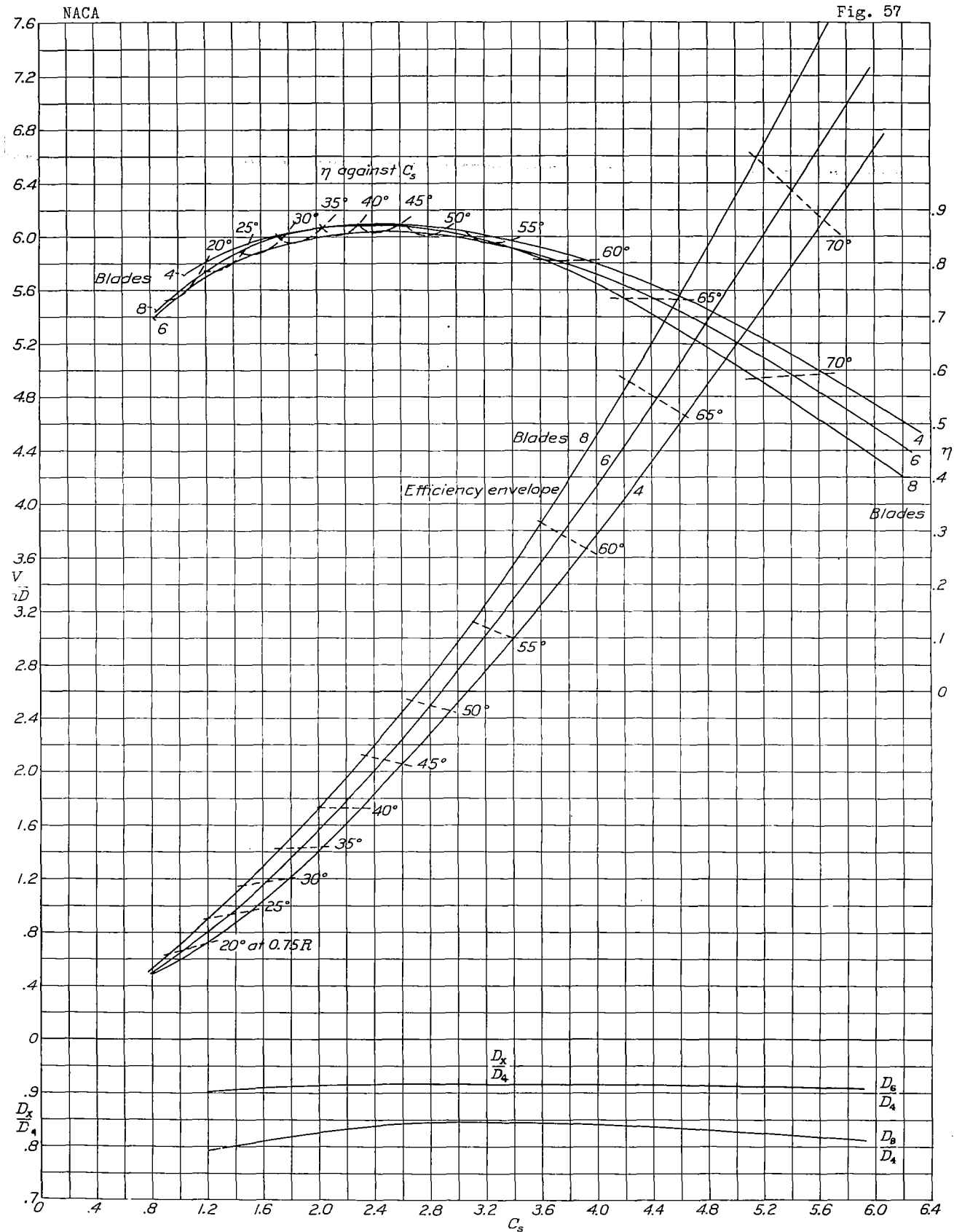


Figure 57.-Composite skeleton C_s chart for four -, six -, and eight blades. Dual rotation.
Propellers 3155-6 and 3156-6.

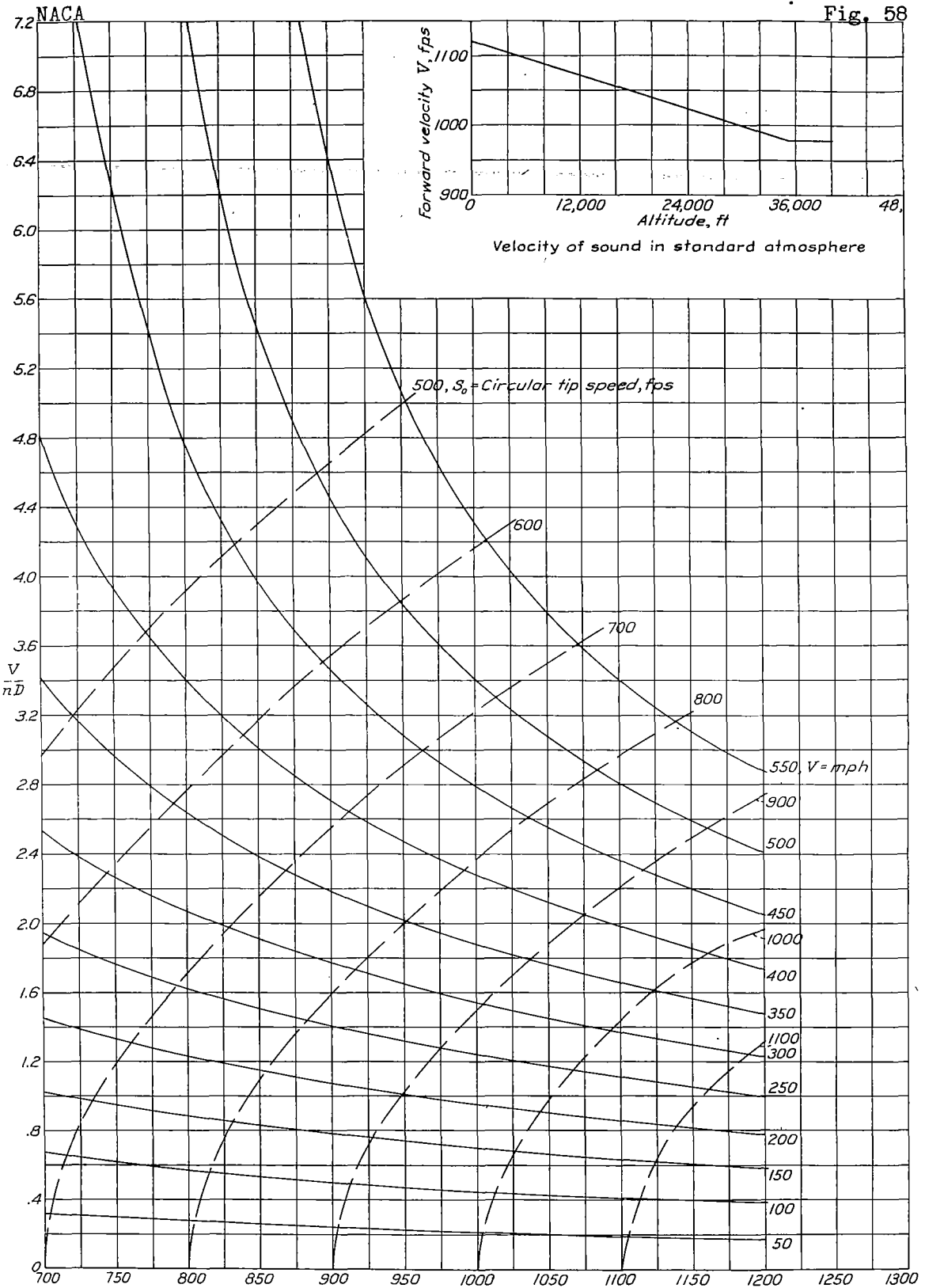


Figure 58.-Relation between helical tip speed, forward speed, and equivalent V/nD . $S_h = \sqrt{S_0^2 + V^2}$